Semi-empirical modeling of abiotic and biotic factors controlling ecosystem respiration across eddy covariance sites

Mirco Migliavacca, Markus Reichstein, Andrew D. Richardson, Roberto Colombo, Mark A. Sutton, Gitta Lasslop, Georg Wohlfahrt, Enrico Tomelleri, Nuno Carvalhais, Alessandro Cescatti, et al.

Semi-empirical modeling of abiotic and biotic factors controlling ecosystem respiration across eddy covariance sites

Journal:	*Global Change Biology*
Manuscript ID:	GCB-10-0015
Wiley - Manuscript type:	Primary Research Articles
Date Submitted by the Author:	07-Jan-2010
Complete List of Authors:	Migliavacca, Mirco; University of Milano-Bicocca, Remote Sensing of Environmental Dynamics; Max Planck Institute for Biogeochemistry, Model Data Integration Group Reichstein, Markus; Max Planck Institute for Biogeochemistry, Model Data Integration Group Richardson, Andrew; Harvard University, Department of Organismic and Evolutionary Biology Colombo, Roberto; University of Milano-Bicocca, Remote Sensing of Environmental Dynamics Sutton, Mark A.; Centre for Ecology and Hydrology, Edinburgh Research Station Lasslop, Gitta; Max Planck Institute for Biogeochemistry, Model Data Integration Group Wohlfahrt, Georg; University of Innsbruck, Institute of Ecology Tomelleri, Enrico; Max Planck Institute for Biogeochemistry, Model Data Integration Group Carvalhais, Nuno; Universidade Nova de Lisboa, Faculdade de Ciências e Tecnologia; Max Planck Institute for Biogeochemistry, Model Data Integration Group Cescatti, Alessandro; European Commission, DG-JRC, Institute for Environment and Sustainability Mahecha, Miguel; Max Planck Institute for Biogeochemistry, Model Data Integration Group; Swiss Federal Institute of Technology-, Department of Environmental Sciences Montagnani, Leonardo; Provincia Autonoma di Bolzano, Agenzia per l'Ambiente, Servizi Forestali Papale, Dario; University of Tuscia, DISAFRI Zaehle, Sönke; Max Planck Institute for Biogeochemistry, Department for Biogeochemical System Arain, M Altaf; McMaster University, School of Geography & Earth Sciences Arneth, Almut; Lund University, 13- Department of Physical Geography and Ecosystems Analysis

	Black, T Andrew; University of British Columbia, Faculty of Land and Food Systems Dore, Sabina; Northern Arizona University, School of Forestry Gianelle, Damiano; Fondazione Edmund Mach, Centro di Ecologia Alpina Helfter, Carole; Centre for Ecology and Hydrology, Edinburgh Research Station Hollinger, David; USDA Forest Service, NE Research Station Kutsch, Werner; Johann Heinrich von Thünen Institut, Institut für Agrarrelevante Klimaforschung Law, Beverly; Oregon State University, College of Forestry Lafleur, Peter M; Trent University, 20- Department of Geography Nouvellon, Yann; CIRAD, Persyst Rebmann, Corinna; Max-Planck Institute for Biogeochemistry, Biogeochemical Processes; University of Bayreuth, Department of Micrometeorology da Rocha, Humberto; Universidade de São Paulo, Dept. of Atmospheric Sciences Rodeghiero, Mirco; Fondazione Edmund Mach, Centro di Ecologia Alpina Olivier, Roupsard; CIRAD, Persyst; Centro Agronómico Tropical de Investigación y Enseñanza, CATIE Sebastià, Maria-Teresa; University of Lleida, Agronomical Engineering School; Forest Technology Centre of Catalonia, Laboratory of Plant Ecology and Botany Seufert, Guenther; Institute for Environment and Sustainability, European Commission, DG-JRC Soussana, Jean-Francoise; Institut National de la Recherche Agronomique van der Molen, Michiel K; University de Boeleaan, Department of Hydrology and Geo-Environmental Sciences
Keywords:	Ecosystem Respiration, Productivity, FLUXNET, Eddy Covariance, Leaf Area Index, Inverse Modeling
Abstract:	In this study we examined ecosystem respiration (RECO) data from 104 sites belonging to FLUXNET, the global network of eddy covariance flux measurements. The main goal was to identify the main factors involved in the variability of RECO: temporally and between sites as affected by climate, vegetation structure and plant functional type (PFT) (evergreen needleleaf, grasslands, etc.). We demonstrated that a model using only climate drivers as predictors of RECO failed to describe part of the temporal variability in the data and that the dependency on gross primary production (GPP) needed to be included as an additional driver of RECO. The maximum seasonal leaf area index (LAIMAX) had an additional effect that explained the spatial variability of reference respiration (the respiration at reference temperature Tref=15°C, without stimulation introduced by photosynthetic activity and without water limitations), with a statistically significant linear relationship ($r^2=0.52$ $p<0.001$, $n=104$) even within each PFT. Besides LAIMAX, we found that the reference respiration may be explained partially by total soil carbon content. For undisturbed temperate and boreal forest a negative control of the total nitrogen deposition on the reference respiration was also identified. We developed a new semi-empirical model incorporating abiotic factors (climate), recent productivity (daily GPP), general site productivity and canopy structure (LAIMAX) which performed well in predicting the spatio-temporal variability of RECO, explaining >70% of the variance for most vegetation types. Exceptions include tropical and Mediterranean broadleaf forests and deciduous

	broadleaf forests. Part of the variability in respiration that could not be described by our model could be attributed to a range of factors, including phenology in deciduous broadleaf forests and management practices in grasslands and croplands.

Semi-empirical modeling of abiotic and biotic factors controlling ecosystem respiration across eddy covariance sites

Mirco Migliavacca[1,2], Markus Reichstein[2], Andrew D. Richardson[3], Roberto Colombo[1], Mark A. Sutton[4], Gitta Lasslop[2], Georg Wohlfahrt[5], Enrico Tomelleri[2], Nuno Carvalhais[6,2], Alessandro Cescatti[7], Miguel D. Mahecha[2,8], Leonardo Montagnani[9], Dario Papale[10] , Sönke Zaehle [11], Altaf Arain[12], Almut Arneth[13], T. Andrew Black[14], Sabina Dore[15], Damiano Gianelle[16], Carole Helfter[4], David Hollinger[17], Werner L. Kutsch[18], Beverly E. Law[19], Peter M. Lafleur[20], Yann Nouvellon[21], Corinna Rebmann[22,23], Humberto Ribeiro da Rocha[24], Mirco Rodeghiero[16], Olivier Roupsard[21,25], Maria-Teresa Sebastià[26,27], Guenther Seufert[7], Jean-Francoise Soussana[28], Michiel K. van der Molen[29]

1- Remote Sensing of Environmental Dynamics Laboratory, DISAT, University of Milano-Bicocca, Milano, Italy.
2- Model Data Integration Group, Max Planck Institute for Biogeochemistry, Jena, Germany.
3- Department of Organismic and Evolutionary Biology, Harvard University, Cambridge MA, USA.
4- Centre for Ecology and Hydrology, Edinburgh Research Station, Bush Estate, Penicuik, Midlothian, Scotland, EH26 0QB, UK.
5- Institut für Ökologie, Universität Innsbruck, Innsbruck, Austria.
6- Faculdade de Ciências e Tecnologia, FCT, Universidade Nova de Lisboa, 2829-516, Caparica, Portugal.
7- European Commission, DG-JRC, Institute for Environment and Sustainability, Climate Change Unit, Via Enrico Fermi 2749, T.P. 050, 21027 Ispra (VA), Italy.
8- Department of Environmental Sciences, Swiss Federal Institute of Technology-ETH Zurich, 8092 Zurich, Switzerland.
9- Agenzia Provinciale per l'Ambiente, Via Amba-Alagi 5, 39100 Bolzano, Italy.
10- DISAFRI, University of Tuscia, via C. de Lellis, 01100 Viterbo Italy.
11- Department for Biogeochemical System, Max Planck Institute for Biogeochemistry, Jena, Germany.
12- McMaster University, School of Geography & Earth Sciences, 1280 Main Street West, Hamilton, ON, L8S 4K1, Canada.
13- Department of Physical Geography and Ecosystems Analysis, Lund University, Sölvegatan 12, SE-223 62 Lund, Sweden.
14- Faculty of Land and Food Systems, University of British Columbia, Vancouver, BC, Canada.
15- Department of Biological Sciences and Merriam-Powell Center for Environmental Research, Northern Arizona University, Flagstaff, Arizona, USA.
16- IASMA Research and Innovation Centre, Fondazione E. Mach, Environment and Natural Resources Area, San Michele all'Adige, I-38040 Trento, Italy
17- USDA Forest Service, NE Research Station, Durham, NH, USA
18- Johann Heinrich von Thünen Institut (vTI), Institut für Agrarrelevante Klimaforschung, Braunschweig, Germany
19- College of Forestry, Oregon State University, 97331-5752 Corvallis, OR, USA
20- Department of Geography, Trent University, Peterborough, ON K 9J 7B8, Canada.
21- CIRAD, Persyst, UPR80, TA10/D, 34398 Montpellier Cedex 5, France.
22- University of Bayreuth, Department of Micrometeorology, Bayreuth, Germany.
23- Max Planck Institute for Biogeochemistry, Jena, Germany.
24- Departamento de Ciências Atmosféricas/IAG/Universidade de São Paulo, Rua do Matão, 1226 - Cidade Universitária - São Paulo, SP - Brasil.

25- CATIE, Centro Agronómico Tropical de Investigación y Enseñanza, Turrialba Costa Rica.
26- Laboratory of Plant Ecology and Botany. Forest Technology Centre of Catalonia, Solsona, Spain.
27- Agronomical Engineering School, University of Lleida, E-25198 Lleida, Spain.
28- INRA, Institut National de la Recherche Agronomique, Paris, France.
29- Department of Hydrology and Geo-Environmental Sciences, VU-University, de Boeleaan 1085, 1081 HV Amsterdam, The Netherlands.

Corresponding author:
Mirco Migliavacca
Remote Sensing of Environmental Dynamics
Laboratory, DISAT, University of Milano-Bicocca, P.zza della Scienza 1, 20126
Milan, Italy. Tel.: +39 0264482848; fax: +39 0264482895.
E-mail address: m.migliavacca1@campus.unimib.it

Abstract

In this study we examined ecosystem respiration (R_{ECO}) data from 104 sites belonging to FLUXNET, the global network of eddy covariance flux measurements. The main goal was to identify the main factors involved in the variability of R_{ECO}: temporally and between sites as affected by climate, vegetation structure and plant functional type (PFT) (evergreen needleleaf, grasslands, etc.).

We demonstrated that a model using only climate drivers as predictors of R_{ECO} failed to describe part of the temporal variability in the data and that the dependency on gross primary production (GPP) needed to be included as an additional driver of R_{ECO}. The maximum seasonal leaf area index (LAI_{MAX}) had an additional effect that explained the spatial variability of reference respiration (the respiration at reference temperature Tref=15°C, without stimulation introduced by photosynthetic activity and without water limitations), with a statistically significant linear relationship (r^2=0.52 $p<0.001$, n=104) even within each PFT. Besides LAI_{MAX}, we found that the reference respiration may be explained partially by total soil carbon content. For undisturbed temperate and boreal forest a negative control of the total nitrogen deposition on the reference respiration was also identified.

We developed a new semi-empirical model incorporating abiotic factors (climate), recent productivity (daily GPP), general site productivity and canopy structure (LAI_{MAX}) which performed well in predicting the spatio-temporal variability of R_{ECO}, explaining >70% of the variance for most vegetation types. Exceptions include tropical and Mediterranean broadleaf forests and deciduous broadleaf forests. Part of the variability in respiration that could not be described by our model could be attributed to a range of factors, including phenology in deciduous broadleaf forests and management practices in grasslands and croplands.

Keywords: Ecosystem Respiration, Productivity, FLUXNET, Eddy Covariance, Leaf Area Index, Inverse Modeling

Introduction

Respiration of terrestrial ecosystems (R_{ECO}) is one of the major fluxes in the global carbon cycle and its responses to environmental change is important for understanding climate-carbon cycle interactions (e.g. Cox *et al.*, 2000, Houghton *et al.*, 1998). It has been hypothesized that relatively

small climatic changes may impact respiration with the effect of rivalling the annual fossil fuel loading of atmospheric CO_2 (Jenkinson *et al.*, 1991, Raich & Schlesinger, 1992).

Recently, efforts have been made to mechanistically understand how temperature and other environmental factors affect ecosystem and soil respiration, and various modeling approaches have been proposed (e.g. Davidson *et al.*, 2006a, Lloyd & Taylor, 1994, Reichstein & Beer, 2008, Reichstein *et al.*, 2003a). Nevertheless, the description of the conceptual processes and the complex interactions controlling R_{ECO} are still under intense research and this uncertainty is still hampering bottom-up scaling to larger spatial scales (e.g. regional and continental) which is one of the major challenges for biogeochemists and climatologists.

Heterotrophic and autotrophic respiration in both data-oriented and process-based biogeochemical models are usually described as a function of air or soil temperature and occasionally soil water content (e.g. Lloyd & Taylor, 1994, Reichstein *et al.*, 2005, Thornton *et al.*, 2002), although the functional form of these relationships varies from model to model. These functions represent the dominant role of reaction kinetics, possibly modulated or confounded by other environmental factors such as soil water content or precipitation, which some model formulations include as a secondary effect (e.g. Carlyle & Ba Than, 1988, Reichstein *et al.*, 2003a, Richardson *et al.*, 2006).

A large number of statistical, climate-driven models of ecosystem and soil respiration have been tested and compared using data from individual sites (Del Grosso *et al.*, 2005, Janssens & Pilegaard, 2003, Richardson & Hollinger, 2005, Savage *et al.*, 2009), multiple sites (Falge *et al.*, 2001, Rodeghiero & Cescatti, 2005), and from a wide range of models compared across different ecosystem types and measurement techniques (Richardson et al., 2006).

Over the course of the last decades, the scientific community has debated the role of productivity in determining ecosystem and soil respiration. Several authors (Bahn *et al.*, 2008, Curiel Yuste *et al.*, 2004, Davidson *et al.*, 2006a, Janssens *et al.*, 2001, Reichstein *et al.*, 2003a, Valentini *et al.*, 2000) have discussed and clarified the role of photosynthetic activity, vegetation productivity and their relationship with respiration.

Linking photosynthesis and respiration might be of particular relevance when modelling R_{ECO} across biomes or at the global scale. Empirical evidence for the link between GPP and R_{ECO} is reported for most, if not all, ecosystems: grassland (e.g. Bahn *et al.*, 2008, Bahn *et al.*, 2009, Craine *et al.*, 1999, Hungate *et al.*, 2002), crops (e.g. Kuzyakov & Cheng, 2001, Moyano *et al.*, 2007), boreal forests (Gaumont-Guay *et al.*, 2008, Hogberg *et al.*, 2001) and temperate forests, both deciduous (e.g. Curiel-Yuste *et al.*, 2004, Liu *et al.*, 2006) and evergreen (e.g. Irvine *et al.*, 2005).

Moreover, several authors have found a time lag between productivity and respiration response. This time lag depends to the vegetation structure it is related to the translocation time of assimilates from aboveground to belowground organs through the phloem. Although the existence of a time lag is still under debate, it has been found to be a few hours in grasslands, and croplands and a few days in forests (Baldocchi *et al.*, 2006, Knohl & Buchmann, 2005, Moyano *et al.*, 2008, Savage *et al.*, 2009).

While the link between productivity and respiration appears to be clear, to our knowledge, few model formulations include the effect of productivity or photosynthesis as a biotic driver of respiration and these models are mainly developed for the simulation of soil respiration using a relatively small data set of soil respiration measurements (e.g. Hibbard *et al.*, 2005, Reichstein *et al.*, 2003a).

In this context, the increasing availability of ecosystem carbon, water and energy flux measurements collected by means of the eddy covariance technique (e.g. Baldocchi, 2008) over different plant functional types (PFTs) at more than 400 research sites, represents an useful tool for understanding processes and interactions behind carbon fluxes and ecosystem respiration. These data serve as a backbone for bottom-up estimates of continental carbon balance components (e.g. Ciais *et al.*, 2005, Papale & Valentini, 2003, Reichstein *et al.*, 2007) and for ecosystem model development, calibration and validation (e.g. Baldocchi, 1997, Hanson *et al.*, 2004, Law *et al.*, 2000, Owen *et al.*, 2007, Reichstein *et al.*, 2003b, Reichstein *et al.*, 2002, Verbeeck *et al.*, 2006). The database includes a number of added products such as gap-filled net ecosystem exchange (NEE), gross primary productivity (GPP), ecosystem respiration (R_{ECO}) and meteorological drivers (air temperature, radiation, precipitation etc) aggregated at different time-scale (e.g. half-hourly, daily, annual) and consistent for data treatment (Papale *et al.*, 2006, Reichstei *et al.*, 2005)

In this paper we analyze with a semi-empirical modeling approach the R_{ECO} at 104 different sites belonging to the FLUXNET database with the primary objective of synthesizing and identifying the main factors controlling *i*) the temporal variability of R_{ECO}, *ii*) the between-site (spatial) variability and *iii*) to provide a model which can be used for diagnostic up-scaling of R_{ECO} from eddy covariance flux sites to large spatial scales.

Specifically, the analysis and the model development followed these two steps:

1. we developed a semi-empirical R_{ECO} model site by site (site-by-site analysis) with the aim of clarifying if and how GPP should be included into a model for improving the description of R_{ECO} and which factors are best suited for describing the spatial variability of reference respiration (i.e. the daily R_{ECO} at the reference temperature without moisture limitations). We follow these three steps:

- the analysis of R_{ECO} data was conducted by using a purely climate driven model: *'TP Model'* (Raich et al., 2002). The accuracy of the model and the main bias were analyzed and discussed;
- we evaluated the inclusion of biotic factors (i.e. GPP) as drivers of R_{ECO}. A range of different model formulations, which differ mainly in regard to the functional responses of R_{ECO} to photosynthesis, were tested in order to identify the best model formulation for the daily description of R_{ECO} at each site;
- we analyzed variability of the reference respiration estimated at each site with the aim of identifying, among the different site characteristics, one or more predictors of the spatial variability of this crucial parameter. This can be extremely useful for the application of the model at large spatial scale;

2. we optimized the developed model for each PFT (PFT analysis) with the aim of generalizing the model parameters in a way that can be useful for diagnostic, PFT-based, up-scaling of R_{ECO}. The accuracy of the model was assessed by a cross-validation technique and the main weak points of model were critically evaluated and discussed.

Material and Methods

Data set

The data used in this analysis is based on the dataset from the FLUXNET (www.fluxdata.org) eddy covariance network (Baldocchi, 2008, Baldocchi *et al.*, 2001). The analysis was restricted to 104 sites (cf. Table in Appendix I and II) on the basis of the ancillary data availability (i.e. only sites containing at least both leaf area index (LAI) of understorey and overstorey were selected) and of the time series length (all sites containing at least one year of carbon fluxes and meteorological data of good quality data were used). Further, we only analyzed those sites for which the relative standard error of the estimates of the model parameters E_0 (activation energy) and reference respiration (R_0) (please see further sections for more details on the meaning of parameters) were less than 50% and where E_0 estimates were within an acceptable range (0–450 K).

The latitude spans from 71.32° at the Alaska Barrow site (US-Brw) to -21.62° at the Sao Paulo Cerrado (BR-Sp1). The climatic regions include tropical to arctic.

All the main PFTs as defined by the IGBP (International Geosphere-Biosphere Programme) were included in this study: the selected sites included 28 evergreen needleleaf forests (ENF), 17

deciduous broadleaf forests (DBF), 16 grasslands (GRA), 11 croplands (CRO), 8 mixed forests (MF), 5 savannas (SAV), 9 shrublands (SHB), 7 evergreen broadleaved forests (EBF) and 3 wetlands (WET). Due to limited number of sites and their similarity, the class SAV included both the sites classified as savanna (SAV) and woody savannas (WSA), while the class SHB included both the open (OSH) and closed (CSH) shrubland sites. For abbreviations and symbols refer to Appendix III.

Daily R_{ECO}, GPP and the associated uncertainties of NEE data, together with daily meteorological data such as mean air temperature (T_A) and 30-day precipitation running average (P), were downloaded from the FLUXNET database.

At each site data are storage corrected, spike filtered, u_*-filtered according to Papale et al. (2006) and subsequently gap-filled and partitioned as described by Reichstein et al. (2005). Only days containing both meteorological and daily flux data with a percentage of gap-filled half hours below 15% were used for this analysis. The median of the u_* threshold applied in the FLUXNET database for the site-years used in the analysis are listed in the Appendix II. The average of the median u_* values are lower for short canopies (e.g. for grasslands 0.075±0.047 ms^{-1}) and higher for tall canopies (e.g. for evergreen needleleaf forests 0.221 ±0.115 ms^{-1}).

Along with fluxes and meteorological data, main ancillary data such as maximum ecosystem LAI (overstory and understory for forest sites) (LAI_{MAX}), LAI of overstory ($LAI_{MAX,o}$), stand age for forests (StandAge), total soil carbon stock (SoilC) and the main information about disturbance (date of cuts, harvesting) were also downloaded from the database. Total atmospheric nitrogen deposition (N_{depo}) is based on the atmospheric chemistry transport model *TM3* (Rodhe et al., 2002) and calculated at 1°x1° resolution. These data are grid-average downward deposition velocities and do not account for vegetation effects. The data used for the selected sites are shown in the Appendix II.

Development of the ecosystem respiration model

Site-by-site analysis – TP Model description

For the analysis of R_{ECO} we started from a widely used climate-driven model: '*TP Model*' (Eq. 1) proposed by Raich et al. (2002) and further modified by (Reichstein *et al.*, 2003a). Here we used the '*TP Model*' for the simulation of R_{ECO} at the daily time-step using as abiotic drivers daily T_A and P:

$$R_{ECO} = R_{ref} \cdot f(T_A) \cdot f(P) \quad (1)$$

where R_{ref} (gC $m^{-2}day^{-1}$) is the ecosystem respiration at the reference temperature (T_{ref}, K) without water limitations. $f(T_A)$ and $f(P)$ are functional responses of R_{ECO} to air temperature and precipitation, respectively.

Here temperature dependency $f(T_A)$ is changed from the Q_{10} model to an Arrhenius type equation (Eq. 2). E_0 (K) is the activation energy parameter and represents the ecosystem respiration sensitivity to temperature, T_{ref} is fixed at 288.15 K (15°C) and T_0 is fixed at 227.13 K (-46.02°C):

$$f(T_A) = e^{E_0\left(\frac{1}{T_{ref}-T_0}-\frac{1}{T_A-T_0}\right)} \quad (2)$$

We refine the approach of Reichstein *et al.* (2003) and propose a reformulation of the response of R_{ECO} to precipitation (Eq. 3), where k (mm) is the half saturation constant of the hyperbolic relationship and α is the response of R_{ECO} to null P.

$$f(P) = \frac{\alpha k + P(1-\alpha)}{k + P(1-\alpha)} \quad (3)$$

Although soil water content is widely recognized as the best descriptor of soil water availability, we preferred to use precipitation since the model developed is oriented to up-scaling and soil water maps are more affected by uncertainty than precipitation maps.

The model parameters – R_{REF}, E_0, α, k - were estimated for each site in order to evaluate the accuracy of the climate-driven model. At each site the Pearson's correlation coefficient (r) between *'TP Model'* residuals (R_{ECO} observed minus R_{ECO} modelled) and GPP was also computed.

Site-by-site analysis - Effect of productivity on the temporal variability of R_{ECO}

The role of GPP, as an additional biotic driver of R_{ECO} that has been included into Eq. 1, was analysed at each site using three different formulations of the dependency of ecosystem respiration on productivity $f(GPP)$:

Linear response: $$f(GPP) = k_2 \cdot GPP \quad (4)$$

Exponential response: $$f(GPP) = R_2 \cdot \left(1 - e^{-k_2 \cdot GPP}\right) \quad (5)$$

Michaelis-Menten: $$f(GPP) = \frac{R_{max} \cdot GPP}{h_{R_{max}} + GPP} \quad (6)$$

Beside the linear dependency the exponential and Michaelis-Menten responses were tested. According to different authors (e.g. Hibbard et al., 2005, Reichstein et al., 2007) we hypothesized that respiration might saturate at high productivity rates in a similar way to the Michaelis-Menten enzyme kinetics. This saturation can also occur by a transition of carbon limitation to other limitations. The exponential curve was used as another formulation of a saturation effect.

We tested two different schemes for the inclusion of *f*(GPP) (Eqs. 4, 5, 6) in the *'TP Model'* (Eq.1):

1) *f*(GPP) was included by replacing the reference respiration at reference temperature (R_{ref} in Eq. 1) with the sum of a new reference respiration (R_0) and the f(GPP):

$$R_{ref} = R_0 + f(GPP) \qquad (7)$$

2) *f*(GPP) was included as an additive effect into the *'TP Model'*. In this case one part of ecosystem respiration is purely driven by biotic factors (e.g. independent from temperature) and the other one by abiotic ones.

In Table 1, R_0 is the new reference respiration term (i.e. ecosystem respiration at T_{ref}, when the GPP is null and the ecosystem is well watered). This quantity is considered to be an indicator of the ecosystem respiration of the site, strictly related to site conditions, history and characteristics, while k_2, R_2, R_{max} and h_{Rmax} describe the assumed functional response to GPP**.**

[TABLE1]

The model parameters - R_0, E_0, α, k and the parameters of *f*(GPP) - were estimated for each site in order to evaluate which model formulation best describes the temporal variability of R_{ECO}.

With the aim of confirming the existence of a time lag between photosynthesis and the respiration response we ran the model with different time lagged GPP time-series ($GPP_{lag,i}$), starting from the GPP estimated on the same day ($GPP_{lag,0}$), and considering daily increments back to GPP estimated one week before the measured R_{ECO} ($GPP_{lag,7}$).

GPP and R_{ECO} estimated with the partitioning method used in the FLUXNET database are derived from the same data (i.e. GPP=R_{ECO}-NEE) and this may to some extent introduce spurious correlation between these two variables. In literature two different positions on that can be found: Vickers *et al.*, (2009) argue that there is a spurious correlation between GPP and R_{ECO} when these component fluxes are jointly estimated from the measured NEE (i.e. as estimated in the FLUXNET database). Lasslop *et al.*, 2009 demonstrated that, when using daily sums or further aggregated data,

self-correlation is important because of the error in R_{ECO} rather than because R_{ECO} being a shared variable for the calculation of GPP.

Lasslop *et al.*, 2010 further suggested a 'quasi'-independent GPP and R_{ECO} estimates (GPP_{LASS} and $R_{ECO\text{-}LASS}$). The method by Lasslop *et al.,* (2010) do not compute GPP as a difference, but derive R_{ECO} and GPP from quasi-disjoint NEE data subsets. Hence, if existing, spurious correlations is minimized.

To understand whether our results are affected or not by the 'spurious' correlation between GPP and R_{ECO} estimated in FLUXNET, we also performed the analysis using the GPP and R_{ECO} estimated by the partitioning method of Lasslop *et al.*, (2010). The details of the analysis are described in the Appendix IV. The results obtained confirmed (Appendix IV) that the data presented and discussed in follow are not influenced by the possible 'spurious' correlation between R_{ECO} and GPP reported in the FLUXNET data set.

Site-by-site analysis – Spatial variability of reference respiration (R_0)

Once the best model formulation was defined, we analyzed the site-by-site (i.e. spatial) variability of R_0: the relationships between the estimated R_0 at each site and site-specific ancillary data were tested, including LAI_{MAX}, $LAI_{MAX,o}$, N_{depo}, SoilC and Age. Leaf mass per unit area and aboveground biomass were not considered because these are rarely reported in the database for the sites studied and poorly correlated with spatial variability of soil respiration, as reported by Reichstein et al. (2003a). In this analysis the sites with incomplete site characteristics were removed (Age was considered only for the analysis of forest ecosystems). On the basis of this analysis the model was reformulated by adding the explicit dependency of R_0 on the site characteristics that best explained its variability.

PFT–Analysis

In this phase we tried to generalize the model parameters in order to obtain a parameterization useful for diagnostic PFT-based up-scaling. For this reason model parameters were estimated including all the sites for each PFT at the same time. The dependency of R_0 was prescribed as a function of site characteristics that best explain the spatial R_0 variability within each PFT class.

The model was corroborated with two different cross-validation methods:

1) Training/evaluation splitting cross-validation: one site at a time was excluded using the remaining subset as the training set and the excluded one as the validation set. The model was fitted against each training set and the resulting parameterization was used to predict the R_{ECO} of the excluded site.
2) *k*-fold cross-validation: the whole data set for each PFT was divided into *k* randomly selected subsets (*k*=15) called a fold. The model is fitted against *k-1* remaining folds (training set) while the excluded fold (validation set) was used for model evaluation. The cross-validation process was then repeated *k* times, with each of the *k* folds used exactly once as the validation set.

For each validation set of the cross-validated model statistics were calculated (see 'Statistical Analysis' section). Finally, for each PFT we averaged the cross-validated statistics to produce a single estimation of model accuracy in prediction.

Statistical analysis

Model parameters estimates

Model parameters were estimated using the Levenberg-Marquardt method, implemented in the data analysis package "PV-WAVE 8.5 advantage" (Visual Numerics, 2005), a non-linear regression analysis that optimize model parameters finding the minimum of a defined cost function. The cost function used here is the sum of squared residuals weighted for the uncertainty of the observation (e.g. Richardson et al., 2005). The uncertainty used here is an an estimate of the random error associated with the night-time fluxes (from which R_{ECO} is derived).

Model parameter standard errors were estimated using a bootstrapping algorithm with N=500 random re-sampling with replacement of the dataset. As described by Efron and Tibshirani (1993), the distribution of parameter estimates obtained provided an estimate of the distribution of the true model parameters.

Best model formulation selection

For the selection of the 'best' model from among the six different formulations listed in Table 1 and the *'TP Model'* we used the approach of the information criterion developed by Akaike (1973) which is considered a useful metric for model selection (Anderson *et al.*, 2000, Richardson *et al.*,

2006). In this study the Consistent Akaike Information Criterion (cAIC, eq. 8) was preferred to the AIC because the latter is biased with large datasets (Shono, 2005) tending to select more complicated models (e.g. many explanatory variables exist in regression analysis):

$$cAIC = -2\log L(\Theta) + p[\log(n) + 1] \quad (8)$$

where $L(\Theta)$ is the within samples residual sum of squares, p is the number of unknown parameters and n is the number of data (i.e. sample size). Essentially, when the dimension of the data set is fixed, cAIC is a measure of the trade-off between the goodness of fit (model explanatory power) and model complexity (number of parameters), thus cAIC selects against models with an excessive number of parameters. Given a data set, several competing models (e.g different model formulations proposed in Table 1) can be ranked according to their cAIC, with the formulation having the lowest cAIC being considered the best according to this approach.

For the selection of the best set of predictive variables of R_0 we used the stepwise AIC, a multiple regression method for variable selection based on the AIC criterion (Venables & Ripley, 2002, Yamashita *et al.*, 2007). The stepwise AIC was preferred to other stepwise methods for variable selection since can be applied to non normally distributed data (Yamashita *et al.*, 2007).

Evaluation of model accuracy

Model accuracy was evaluated by means of different statistics according to Janssen and Heuberger (1995): RMSE (Root Mean Square Error), EF (modelling efficiency), determination coefficient (r^2) and MAE (Mean Absolute Error). In particular EF is a measure of the coincidence between observed and modelled data and it is sensitive to systematic deviation between model and observations. EF can range from $-\infty$ to 1. An EF of 1 corresponds to a perfect agreement between model and observation. An EF of 0 (EF = 0) indicates that the model is as accurate as the mean of the observed data, whereas a negative EF means that observed mean is a better predictor than the model. In the PFT-analysis for each validation set the cross-validated statistics were calculated. The average of cross-validated statistics were calculated for each PFT both for the training/evaluation splitting (EF_{cv}, $RMSE_{cv}$, r^2_{cv}) and for the *k-fold* cross-validation ($EF_{kfold\text{-}cv}$, $RMSE_{kfold\text{-}cv}$, $r^2_{kfold\text{-}cv}$).

Results

Site-by-Site analysis

TP Model Results

The RMSE and EF obtained with *'TP Model'* fitting (Table 2) showed a within-PFT-average EF ranging from 0.38 for SAV to 0.71 for ENF and an RMSE ranging from 0.67 for SHB to 1.55 gC m^{-2} d^{-1} for CRO.

[TABLE 2]

The importance of productivity is highlighted by residual analysis. A significant positive correlation between the *'TP Model'* residuals (z) and the GPP was observed with a systematic underestimation of respiration when the photosynthesis (i.e. GPP) was intense.

In Fig. 1a, the mean r between the residuals and GPP for each PFT as a function of the time lag is summarised.

The lowest correlation was observed for wetlands (r=0.29±0.14). The mean r is higher for herbaceous ecosystems such as grasslands and croplands (0.55±0.11 and 0.63±0.18, respectively) than for forest ecosystems (ENF, DBF, MF, EBF) which behaved in the same way (Fig. 1a), with a r ranging from 0.35±0.13 for ENF to 0.45±0.13 for EBF. No time lag was observed with the residuals analysis.

Gross Primary Production as driver of R_{ECO}

The effect of GPP as an additional driver of R_{ECO} was analyzed at each site by testing 6 different models with the three different functional responses (Eqs. 4, 5 and 6) of respiration to GPP (Tab. 1). The model ranking based on the cAIC calculated for each different model formulation at each site showed agreement in considering the models using the linear dependency of R_{ECO} on GPP ('LinGPP') as the best model formulation (Tab. 2), since the cAICs obtained with 'LinGPP' were lower than those obtained with all the other formulations. This model ranking was also maintained when analysing each PFT separately, except for croplands in which the 'addLinGPP' formulation provided the minimum cAIC although the difference between the average cAIC estimated for the

two model formulations was almost negligible (cAIC was 38.22 ± 2.52 and 38.26 ± 2.45 for 'addLinGPP' and 'LinGPP', respectively) and the standard errors of parameter estimates were lower for the 'LinGPP' formulation. In general, the cAIC obtained at all sites with the 'LinGPP' model formulation (39.50 [37.50 – 42.22], in squared parentheses the first and third quartile are reported) were lower than the ones obtained with the *'TP Model'* (41.08 [39.02 - 44.40]), although the complexity of the latter is lower (one parameter less). On this basis we considered the 'LinGPP' as the best one model formulation.

The statistics of model fitting obtained with the 'LinGPP' model formulation are reported in Table 2. The model optimized site by site showed a within-PFT-average of EF between 0.58 for EBF to 0.85 for WET with an RMSE ranging from 0.53 for SAV to 1.01 gC m^{-2} day^{-1} for CRO. On average EF was higher than 0.65 for all the PFTs except for EBF. In terms of improvement of statistics, the use of 'LinGPP' in the *'TP Model'* led to a reduction of the RMSE from 13.4 % for shrublands to almost one third for croplands (34.8%), grasslands (32.5%) and savanna (32.0%) with respect to the statistics corresponding to the purely climate driven *'TP Model'*.

[FIGURE 1]

No time lag between photosynthesis and respiration response was detected. In fact using $GPP_{lag,-i}$ as a model driver we observed a general decrease in mean model performances for each PFT (i.e. decrease of EF and increase of RMSE) for increasing *i* values (i.e. number of days in which the GPP was observed before the observed R_{ECO}). The only exception were DBFs in which we found a time lag between the GPP and R_{ECO} response of 3 days as shown by the peak in average EF and by the minimum in RMSE in Fig. 1b, although the differences were not statistically significant.

Spatial variability of reference respiration rates

The reference respiration rates (R_0) estimated site by site with the 'LinGPP' model formulation represent the daily ecosystem respiration at each the site at a given temperature (i.e. 15°C), without water limitation and carbon assimilation. Hence, R_0 can be consider the respiratory potential of a particular site. R_0 assumed highest values for the ENF (3.01±1.35 gC m^{-2} day^{-1}) while the lowest values were found for SHB (1.49±0.82 gC m^{-2} day^{-1}) and WET (1.11 ±0.17 gC m^{-2} day^{-1}), possibly reflecting lower carbon pools for shrublands or lower decomposition rates due to anoxic conditions or carbon stabilization for wetlands.

By testing the pairwise relationship between R_0 and different site characteristics we found that the ecosystem LAI_{MAX} showed the closest correlation with R_0 ($R_0=0.44(0.04)LAI_{MAX}+0.78(0.18)$, $r^2=0.52$, $p<0.001$, n=104, in parentheses standard errors of model parameters estimates were reported), thus LAI_{MAX} was the best explanatory variable of the retrieved R_0 variability (Fig 2a). Conversely, $LAI_{MAX,o}$ correlated weakly ($r^2=0.40$, $p<0.001$, n=104) with R_0 (Fig. 2b) indicating that, for forest sites, understorey LAI must be also taken into account. A very weak correlation was found with SoilC ($r^2=0.09$; $p<0.001$, n=67) and no significant correlation with Age, N_{depo} and T_{MEAN} were found for forest sites (Fig. 2 c-f).

[FIGURE 2]

The multiple regression analysis conducted with the stepwise AIC method including simultaneously all sites, showed that the two best predictors of R_0 were LAI_{MAX} and SoilC (Multiple $r^2=0.57$; $p<0.001$; n=68) which were both positively correlated with R_0 (Tab. 3). LAI_{MAX} was the best predictor of spatial variability of R_0 for all sites confirming the results of the pairwise regression analysis above mentioned but the linear model which included the SoilC as additional predictor led to a significant, though small, reduction in the AIC during the stepwise procedure.

Considering only the undisturbed temperate and boreal forest sites (ENF, DBF, MF), the predictive variables of R_0 selected were LAI_{MAX} and N_{depo}. (Multiple $r^2=0.67$; $p<0.001$; n=23). For these sites both LAI_{MAX}, which was still the main predictor of spatial variability of R_0, and N_{depo} controlled the spatial variability of R_0, with N_{depo} negatively correlated to R_0 (Tab. 3). This means that for these sites, once removed the effect of LAI_{MAX}, N_{depo} showed a negative control on R_0 with a reduction of 0.025 gC m^{-2} day^{-1} in reference respiration for an increase of 1 kg N $ha^{-1}year^{-1}$. Considering only the disturbed forest sites we found that SoilC and T_{MEAN} were the best predictors of spatial variability of R_0 (Multiple $R^2= 0.80$, $p<0.001$, n=10).

In Table 5 (left column) the statistics of the pairwise regression analysis between R_0 and LAI_{MAX} for each PFT are reported. The best fitting was obtained with the linear relationship for all PFTs except for deciduous forests for which the best fitting was obtained with the exponential relationship $R_0=R_{LAI=0}(1-e^{-aLAI})$.

[TABLE 3 AND TABLE 4]

PFT-Analysis

Final formulation of the model

On the basis of the aforementioned results, the GPP as well as the linear dependency between R_0 and LAI_{MAX} were included into the *'TP Model'* leading to a new model formulation (Eq 9). The final formulation is basically the *'TP Model'* with the addition of biotic drivers (daily GPP and LAI_{MAX}) and hereafter referred to as *'TPGPP-LAI Model'*, where the suffixes GPP and LAI reflect the inclusion of the biotic drivers in the climate-driven model:

$$R_{ECO} = \left(\underbrace{R_{LAI=0} + a_{LAI} \cdot LAI_{MAX}}_{R_0} + k_2 GPP \right) \cdot e^{E_0 \left(\frac{1}{T_{ref} - T_0} - \frac{1}{T_A - T_0} \right)} \cdot \frac{\alpha k + P(1-\alpha)}{k + P(1-\alpha)} \qquad (9)$$

where the term, $R_{LAI=0} + a_{LAI}\ LAI_{MAX}$, describes the dependency of the basal rate of respiration (R_0 in Table1) on site maximum seasonal ecosystem LAI. Although we found that SoilC and N_{depo} may help to explain the spatial variability of R_0, in the final model formulation we included only the LAI_{MAX}. In fact the model is primarily oriented to the up-scaling and spatial distributed information of SoilC, N_{depo} and disturbance may be difficult to be gathered and usually are affected by high uncertainty.

The parameters $R_{LAI=0}$ and a_{LAI} listed in Table 4 were introduced as fixed parameters in the *'TPGPP-LAI Model'*. For wetlands and mixed forests the overall relationship between LAI_{MAX} and R_0 was used. For wetlands, available sites were insufficient to construct a statistically significant relationship while for mixed forests the relationship was not significant (p=0.146).

PFT specific model parameters (k_2, E_0, k, α) of *'TPGPP-LAI Model'* were then derived using all data from each PFT contemporarily and listed with their relative standard errors in Table 4. No significant differences in parameter values were found when estimating all the parameters simultaneously ($a_{LAI,}$ $R_{LAI=0,}$ k_2, E_0, k, α).

The scatterplots of the observed *vs* modelled annual sums of R_{ECO} are shown in Figure 3, while results and statistics are summarized in Table 5. The model was well able to describe the interannual and intersite variability of the annual sums over different PFTs, with the explained variance varying between 40% for deciduous forests and 97% for shrublands and evergreen broadleaved forests. Considering all sites, the explained variance is 81%, with a mean error of about 17% (132.99 $gCm^{-2}yr^{-1}$) of the annual observed R_{ECO}.

[TABLE 5, FIGURE 3]

Evaluation of model predictions accuracy and weak points

The results obtained with the k-fold and training/evaluation split cross-validation are listed in Table 6.

[TABLE 6]

The r^2_{cv} ranges from 0.52 (for EBF) to 0.80 (for CRO) while the $r^2_{cv,kfold}$ ranges from 0.58 (for DBF) to 0.81 (for GRA). The cross-validated statistics averaged for each PFT are always higher for the *k*-fold than for the training/evaluation splitting cross-validation.

The analysis of model residuals time series of the deciduous broadleaf forest (Fig. 4) showed a systematic underestimation during the springtime development phase and, although less clear, on the days immediately after leaf-fall. A similar behaviour was also found for croplands and grasslands during the days after harvesting or cuts (Fig. 5).

[FIGURE 4,5]

DISCUSSION

Gross primary production as driver of ecosystem respiration

The results obtained with the purely climate-driven model (*'TP Model'*) and the best model formulation selected in the site-by-site analysis (i.e. 'LinGPP', Tab. 1) confirm the strong relationship between carbon assimilation and R_{ECO} highlighting that this relationship must to be included into models aimed to simulate temporal variability of R_{ECO}.

Respiration appears to be strongly driven by the GPP in particular in grasslands, savannas and croplands as already pointed out by several authors in site-level analysis (Bahn *et al.*, 2008, Moyano *et al.*, 2007, Wohlfahrt *et al.*, 2008a, Xu & Baldocchi, 2004). For croplands and grasslands growth respiration is controlled by the amount of photosynthates available and mycorrhizal respiration, which generally constitutes a large component of soil respiration (e.g. Moyano *et al.*, 2007, Kuzyakov & Cheng, 2001).

For wetlands instead the weak relationship between respiration and GPP can be explained by the persistence of anaerobic conditions, decomposition proceeds more slowly with an accumulation of

organic matter on top of the mineral soil layer and respiration is closely related to temperature and water table depth rather than to other factors (Lloyd, 2006).

The lower correlation observed for forest ecosystems than for grasslands and croplands may be due to the higher time for translocation, in trees, of substrates from canopy to roots, related to the rates of phloem carbon transport (Nobel, 2005), which affect the reactivity of the respiration and the release of exudates or assimilates from roots as response to productivity (Mencuccini & Höltta, 2010). This is very often cause of time lags between photosynthesis and respiration response but may justify the reduction of correlation between model residuals and GPP estimated at the same day.

A clear time lag between GPP and R_{ECO} response was not detected. In fact both the residual analysis (Fig. 1a) and the analysis conducted with the *'LinGPP'* model formulation (Fig. 1b) confirmed the general absence of a time lag with the only exception of DBF where a time lag of 3 days was observed although the results were not statistically significant. However, in our opinion, these results do not help to confirm or reject the existence of a time lag for several reasons: *i*) in some studies (e.g. Baldocchi *et al.*, 2006, Tang & Baldocchi, 2005) a lag on the sub-daily time scale was identified and the lags on the daily time scale were attributed to an autocorrelation in weather patterns (i.e. cyclic passage of weather fronts with cycles in temperature or dry and humid air masses) which modulates the photosynthetic activities, since our analysis focused on daily data we were not able to identify the existence of sub-daily time lags; *ii*) lag effects may be more pronounced under favorable growing conditions or during certain periods of the growing season, the analysis of which analysis is out of scope of present study.

Spatial variability of reference respiration rates

The relationship between reference respiration rates (R_0) derived by using the 'LinGPP' model formulation, and LAI_{MAX} (Fig. 2a) is particularly interesting considering that the productivity was already included into the model (i.e. daily GPP is driver of 'LinGPP'). While daily GPP describes the portion of R_{ECO} that originates from recently assimilated carbon (i.e. root/rhizosphere respiration, mychorrizal and growth respiration), LAI_{MAX} is a structural factor which has an additional effect to the short-term productivity and allows to describe the overall ecosystem respiration potential of the ecosystem. For instance, high LAI means increased autotrophic maintenance respiration costs. Moreover LAI_{MAX} can be considered both as an indicator of the general carbon assimilation potential and as an indicator of how much carbon can be released to soil yearly because of litterfall (in particular for forests) and leaf turnover which are directly related to

basal soil respiration (Moyano *et al.*, 2007). At recently disturbed sites, this equilibrium between LAI_{MAX} and soil carbon (through litter inputs) may be broken, for example thinning might lead to a reduction of LAI_{MAX} without any short-term effect on the amount soil carbon, while ploughing in crops or plantations leads solely to a reduction in soil carbon content and not necessarily in LAI. Also in cut or grazed grasslands maximum LAI does not correspond well with litter input because most of this carbon is exported from the site and only partially imported back (as organic manure). This explains why the multiple linear model including LAI_{MAX} and SoilC was selected as the best by the stepwise AIC regression using all the sites contemporarily and why considering only disturbed forest ecosystems we SoilC was selected as best predictor of R_0 (Tab. 3).

Particularly interesting is also the negative control of N_{depo} on R_0 with a reduction of 0.025 gC m^{-2} day^{-1} in R_0 for an increase of 1 kg N $ha^{-1}year^{-1}$. The reduction of heterotrophic respiration in sites with high total nitrogen deposition load was already described in literature and in some site-level analysis and attributable to different processes. For instance soil acidification at high N_{depo} loads may inhibit litter decomposition suppressing the respiration rate (Freeman *et al.*, 2004, Knorr *et al.*, 2005) and increasing in N_{depo} can increase N concentration in litter with a reduction of litter decomposition rates (Berg & Matzner, 1997, Persson *et al.*, 2000) and the consequent reduction of respiration. The latter process is more debated in literature because increased N supply may lead to higher N release from plant litter, which results in faster rates of N cycling and in a stimulation of litter decomposition (e.g. Tietema et al., 1993). However this process is not always clear (e.g. Aerts et al., 2006): in litter mixtures, N-rich and lignin-rich litter may chemically interact with the formation of very decay-resistant complexes (Berg et al., 1993). In addition, litter with a high concentration of condensed tannins may interact with N-rich litter reducing the N release from decomposing litter as described in Hattenschwiler and Vitousek (2000). Thus, the supposed stimulating effects of N addition on N mineralization from decomposing litter may be counteracted by several processes occurring in litter between N and secondary compounds, leading to chemical immobilization of the added N (e.g. Pastor et al., 1987, Vitousek & Hobbie, 2000)

Although the absolute values are a matter of recent debate (De Vries *et al.*, 2008, Magnani *et al.*, 2007, Sutton *et al.*, 2008), it is agreed that N_{depo} stimulates net carbon uptake by temperate and boreal forests. As net carbon uptake is closely related to respiration, once the effect of age is removed, it can be seen that increased N_{depo} has the potential to drive R_{ECO} in either directions. The stimulation of GPP as consequence of the increasing N_{depo} is already include in the model since GPP is a driver. Additionally our analysis suggests that overall an increased total N_{depo} in forests tends to reduce reference respiration. Without considering the effects introduced by N_{depo} in our models we may overestimate R_{ECO}, with a consequent underestimation of the carbon sink strength

of such terrestrial ecosystems. It is also clear that, in managed sites, such interactions apply equally to other anthropogenic nitrogen inputs (fertilizers, animal excreta) (e.g. Galloway *et al.*, 2008). However, considering *i*) that LAI_{MAX} is the most important predictor of R_0, *ii*) that the uncertainty in soil carbon and total nitrogen deposition maps is usually high, *iii*) that the spatial information on disturbance is often lacking and finally *iv*) that our model formulation is oriented to up-scaling issues, we introduced LAI_{MAX} as the only robust predictor of the spatial variability of R_0 in the final model formulation.

The use of LAI_{MAX} is interesting for an up-scaling perspective (e.g. at regional or global scale) since can be derived by remotely sensed vegetation indexes (e.g. normalized vegetation indexes or enhanced vegetation indexes) opening interesting perspectives for the assimilation of remote sensing products into the *'TPGPP-LAI Model'*.

The intercepts of the PFT-based linear regression between R_0 and LAI_{MAX} (Tab.4) suggest that, when the LAI_{MAX} is close to 0 ('ideally' bare soil), the lowest R_0 takes place in arid (EBF,SHB and SAV) and agricultural ecosystems,. The frequent disturbances of agricultural soils (i.e. ploughing and tillage), as well as management, reduce soil carbon content dramatically. In croplands, the estimated R_0 is very low in sites with low LAI. However, with increasing LAI_{MAX}, R_0 shows a rapid increase, thus resulting in high respiration rates for crop sites with high LAI. For EBF, SHB and SAV the retrieved slopes are typical of forest ecosystems, while the intercepts are close to zero because of the lower soil carbon content usually found in these PFTs (Raich & Schlesinger, 1992). Because of the few available sites representing and on similarity in terms of climatic characteristics, savannas, shrublands were grouped.

In grasslands, the steeper slope (a_{LAI}) value found (1.14 ± 0.33) suggests that R_0 increases rapidly with increasing aboveground biomass as already pointed out in literature (Wohlfahrt *et al.*, 2008a, Wohlfahrt *et al.*, 2005a, Wohlfahrt *et al.*, 2005b), i.e. an increase in LAI_{MAX} leads to a stronger increase in R_0 than in other PFTs.

In forest ecosystems, and in particular in evergreen needleleaf and deciduous broadleaf forests, the physical meaning of the higher intercept may be found in less soil disturbance. In boreal forests, the soil carbon stock is generally high even at sites with low LAI_{MAX}, thus maintaining an overall high R_0 which is less dependent on the LAI_{MAX}.

Final formulation of the model and weak points

These results obtained with the *'TPGPP-LAI Model'* cross-validation indicate that the developed model describes the R_{ECO} quite well. In particular results indicate a better description of the

temporal variability of R_{ECO} rather than the spatial variability (or across-site variability). In the training/evaluation splitting in fact, the excluded site for each PFT is modelled using a parameterization derived from the other sites within the same PFT. However, the k-fold is more optimistic than training/evaluation splitting cross-validation because the data set is less disturbed and the calibration and validation datasets are statistically more similar. In the training/evaluation splitting, instead, we exclude one site which is completely unseen by the training optimization procedure.

The derived parameterization of the *'TPGPP-LAI Model'* reported in Table 4 may be considered as an optimized parameterization for the application of the model at large scale (e.g. continental or global). For this application is necessary to link of the developed model with a productivity model and remote sensing products necessary for the estimation of LAI. One of the main advances introduced by this model formulation is the incorporation of GPP and LAI as driver of the ecosystem respiration, which importance in modeling Reco is above discussed. These variables are necessary to improve the description of both the temporal and spatial dynamics or R_{ECO}. These results imply that empirical models used with remote sensing (e.g. Reichstein et al., 2007, Reichstein et al., 2003a, Veroustraete et al., 2002) underestimate the amplitude of R_{ECO} an might lead to wrong conclusions regarding the interpretation of seasonal cycle of the global CO_2 growth rate and annual carbon balance.

The values of the *'TPGPP-LAI Model'* parameters (Tab. 4) related to the precipitation (k, α) indicated a much stronger nonlinearity in the response of R_{ECO} to precipitation for shrublands, wetlands and croplands than for forest ecosystems (Fig. 6). Wetlands and croplands reached saturation (no limitation of water on respiration) after a small rain event underlying their insensitivity to precipitation owing to the presence of water in wetland soils and irrigation in croplands. Grasslands are very sensitive to rain pulse as described in Xu & Baldocchi *et al.* (2004), while savannas and evergreen broadleaved forests showed a strong limitation when rainfall was scanty and f(P) saturation exceed 50 mm $month^{-1}$. The parameters related to GPP dependency (k_2) estimated at PFT level confirm all the results obtained at site level indentifying a clear sensitivity of grasslands and savannah to GPP.

[FIGURE 6]

However, when comparing these parameterizations, it is very likely that a background correlation between precipitation, short-term productivity and soil respiration confused the apparent response of respiration to water availability in the *'TPGPP-LAI Model'*.

Despite the good accuracy, some criticisms and limitations of the *'TPGPP-LAI Model'* were identified, in particular for the deciduous broadleaf forests. The systematic underestimation during

the springtime development phase (Fig 4) is very likely related to the peak in autotrophic respiration due to the intense activity of vegetation during bud burst not described by the model. This hypothesis is confirmed by different authors. For instance, Davidson et al. (2006b) pointed out that during spring development, specific root respiration increases with increasing soil temperature and the concomitant root growth increases the amount of respiring tissue. Moreover, during bud burst also leaf growth, starch mobilisation and increased phloem transport may contribute to this pulse in respiration as shown by Knohl *et al.*, (2003). A systematic underestimation was also observed immediately after the leaf-fall, in which the increase in heterotrophic respiration stimulated by the decomposition of fresh litter was not completely described by the model. These results are in accordance with Davidson et al., (1998) whose showed that the sensitivity of respiration to temperature derived using long-term data input is different from short-term sensitivity because it is confused with other seasonally varying factors. At some DBF sites (US-HA1, DE-Hai, Fig 4) the observed fluxes are lower than the modelled ones during the foliaged period. Also the overall plot for DBF in Fig 4 shows that model values are generally higher than observations. These considerations suggest that the link between phenological models describing overall foliar development (Jolly *et al.*, 2005, Migliavacca *et al.*, 2008) and semi-empirical carbon flux models may be useful for the correction of the long-term sensitivity in active spring or summer periods. Another option is the assimilation of remotely-sensed time series from which the main phenological phases may be derived (e.g. derivative methods) and used for instance for the correction of the temporal variability of model parameters.

We also found a similar behaviour of croplands and grassland during the days after harvesting or cuts, when respiration increased because of the decomposition of organic residues (e.g. grass or crop residues) as depicted for example in Fig. 5. In this case, the model was unable to describe increased respiration following the harvest.

Conclusions

In this study we proposed a model (*'TPGPP-LAI Model'*) for the simulation of R_{ECO} which include the explicit dependency of the respiration to the productivity. We demonstrated that the dependency of respiration on some measure of short-term productivity (e.g. GPP) needs to be included in models simulating ecosystem respiration at regional and global scale in order to improve the description of carbon fluxes and feedbacks between respiration and productivity.

In addition, the general site productivity (using maximum seasonal LAI as a proxy) is another important additional variable which accounts for the spatial variability of reference respiration within different plant-functional types. In other words, the LAI_{MAX} can be used as an indicator of the potential respiration for a specific site related to long-term respiration (i.e. low frequencies of the modelled respiration) while GPP and climate drive the short-term respiration response (i.e. the high frequencies of the modelled respiration). This opens interesting perspectives for assessing properties related to respiration using remote sensing products. Soil carbon content and total atmospheric nitrogen deposition may represent under certain circumstance additional parameters enhancing and suppressing, respectively, reference respiration rates.

We demonstrated that variables related to productivity and site structure are necessary to improve the description of both the temporal and spatial dynamics or R_{ECO}. These results imply that empirical models driven only by climate underestimate the amplitude of R_{ECO} and might lead to wrong conclusions regarding the interpretation of seasonal cycle of the global CO_2 growth rate and annual carbon balance.

We provided a parameterization of the *'TPGPP-LAI Model'* for a PFT-based application of the model at large scale (e.g. continental or global). We have shown that the temporal, spatial and interannual variability of ecosystem respiration can be captured quite well by the proposed model. For this application is necessary a link of the developed model with a productivity model (for GPP estimation) and remote sensing products (necessary for the estimation of LAI). One interesting perspective is the integration of the proposed model formulation into the MODIS-GPP/NPP data stream (e.g MOD17 Light Use Efficiency model) for regional and global estimates of R_{ECO}.

Finally, we observed that a part of ecosystem respiration variance not explained by the model may be related to phenology in forests and to management in grasslands and croplands. For these reasons we consider the link between phenological models and/or remotely-sensed time series of vegetation indexes and respiration models as well as the inclusion of total nitrogen deposition as an additional driver for improving the description of ecosystem respiration in both space and time.

AKNOWLEDGEMENTS

The authors would like to thank all the PIs of eddy-covariance sites, technicians, postdoctoral fellows, research associates, and site collaborators involved in FLUXNET who are not included as co-authors of this paper, without whose work this analysis would not have been possible. This work is the outcome of the La Thuile FLUXNET Workshop 2007, which would not have been possible without the financial support provided by CarboEuropeIP, FAO-GTOS-TCO, iLEAPS, Max Planck Institute for Biogeochemistry, National Science Foundation, University of Tuscia and the US

Department of Energy. Moreover, we acknowledge databasing and technical support from Berkeley Water Center, Lawrence Berkeley National Laboratory, Microsoft Research eScience, Oak Ridge National Laboratory, University of California-Berkeley, University of Virginia. The following networks participated with flux data: AmeriFlux, AfriFlux, AsiaFlux, CarboAfrica, CarboEuropeIP, ChinaFlux, Fluxnet-Canada, KoFlux, LBA, NECC, OzFlux, TCOS-Siberia, USCCC. AmeriFlux grant: US Department of Energy, Biological and Environmental Research, Terrestrial Carbon Program (DE-FG02-04ER63917). Data collection for the US-ARM sites was supported by the Office of Biological and Environmental Research of the U.S. Department of Energy under contract DE-AC02-05CH11231 as part of the Atmospheric Radiation Measurement Program. M.A.S contribution was supported by the Nitro-Europe Project. M.M. was supported by the University of Milano-Bicocca and by the Model Data Integration Group of the Max Planck Institute for Biogeochemistry. We acknowledge the Remote Sensing for Environmental Dynamics Laboratory, LTDA (in particular M. Meroni, L. Busetto and M. Rossini), and the MDI-MPI group (C. Beer and M. Jung) for the fruitful discussions during the data analysis.

References

Aerts R, Van Logtestijn R, Karlsson P S (2006) Nitrogen supply differentially affects litter decomposition rates and nitrogen dynamics of sub-arctic bog species. *Oecologia,* 146, 652-658.

Akaike H (1973) Information theory and an extension of the maximum likelihood principle, Budapest.

Allison V J, Miller R M, Jastrow J D, Matamala R, Zak D R (2005) Changes in soil microbial community structure in a tallgrass prairie chronosequence. *Soil Science Society of America Journal,* **69**, 1412-1421.

Ammann C, Flechard C R, Leifeld J, Neftel A, Fuhrer J (2007) The carbon budget of newly established temperate grassland depends on management intensity. *Agriculture Ecosystems & Environment,* **121**, 5-20.

Anderson D R, Burnham K P, Thompson W L (2000) Null hypothesis testing: Problems, prevalence, and an alternative. *Journal of Wildlife Management,* **64**, 912-923.

Arain a A, Restrepo-Coupe N (2005) Net ecosystem production in a temperate pine plantation in southeastern Canada. *Agricultural and Forest Meteorology,* **128**, 223-241.

Aubinet M, Chermanne B, Vandenhaute M, Longdoz B, Yernaux M, Laitat E (2001) Long term carbon dioxide exchange above a mixed forest in the Belgian Ardennes. *Agricultural and Forest Meteorology,* **108**, 293-315.

Aurela M, Laurila T, Tuovinen J P (2002) Annual CO2 balance of a subarctic fen in northern Europe: Importance of the wintertime efflux. *Journal of Geophysical Research-Atmospheres,* **107**.

Bahn M, Rodeghiero M, Anderson-Dunn M *et al.* (2008) Soil Respiration in European Grasslands in Relation to Climate and Assimilate Supply. *Ecosystems,* **11**, 1352-1367.

Bahn M, Schmitt M, Siegwolf R, Richter A, Bruggemann N (2009) Does photosynthesis affect grassland soil-respired CO2 and its carbon isotope composition on a diurnal timescale? *New Phytologist,* **182**, 451-460.

Baldocchi D (1997) Measuring and modelling carbon dioxide and water vapour exchange over a temperate broad-leaved forest during the 1995 summer drought. *Plant Cell and Environment,* **20**, 1108-1122.

Baldocchi D (2008) Breathing of the terrestrial biosphere: lessons learned from a global network of carbon dioxide flux measurement systems. *Australian Journal of Botany,* **56**, 1-26.

Baldocchi D, Falge E, Gu L H *et al.* (2001) FLUXNET: A new tool to study the temporal and spatial variability of ecosystem-scale carbon dioxide, water vapor, and energy flux densities. *Bulletin of the American Meteorological Society,* **82**, 2415-2434.

Baldocchi D, Tang J W, Xu L K (2006) How switches and lags in biophysical regulators affect spatial-temporal variation of soil respiration in an oak-grass savanna. *Journal of Geophysical Research-Biogeosciences,* **111**.

Berg B, Berg M P, Bottner P *et al.* (1993) Litter mass-loss rates in pine forests of europe and eastern united states - some relationship with climate and litter quality. *Biogeochemistry,* 20, 127-159.

Berg B, Matzner E (1997) Effect of N deposition on decomposition of plant litter and soil organic matter in forest ecosystems. *Environmental Reviews,* **5**, 1–25.

Bergeron O, Margolis H A, Black T A, Coursolle C, Dunn a L, Barr a G, Wofsy S C (2007) Comparison of carbon dioxide fluxes over three boreal black spruce forests in Canada. *Global Change Biology,* **13**, 89-107.

Beringer J, Hutley L B, Tapper N J, Cernusak L A (2007) Savanna fires and their impact on net ecosystem productivity in North Australia. *Global Change Biology,* **13**, 990-1004.

Black T A, Chen W J, Barr a G *et al.* (2000) Increased carbon sequestration by a boreal deciduous forest in years with a warm spring. *Geophysical Research Letters,* **27**, 1271-1274.

Borken W, Savage K, Davidson E A, Trumbore S E (2006) Effects of experimental drought on soil respiration and radiocarbon efflux from a temperate forest soil. *Global Change Biology,* **12**, 177-193.

Carlyle J C, Ba Than U (1988) Abiotic controls of soil respiration beneath an eighteen-year-old Pinus radiata stand in south-eastern Australia. *Journal of Ecology,* **76**, 654–662.

Chiesi M, Maselli F, Bindi M *et al.* (2005) Modelling carbon budget of Mediterranean forests using ground and remote sensing measurements. *Agricultural and Forest Meteorology,* **135**, 22-34.

Ciais P, Reichstein M, Viovy N *et al.* (2005) Europe-wide reduction in primary productivity caused by the heat and drought in 2003. *Nature,* **437**, 529-533.

Clark K L, Gholz H L, Castro M S (2004) Carbon dynamics along a chronosequence of slash pine plantations in north Florida. *Ecological Applications,* **14**, 1154-1171.

Cook B D, Davis K J, Wang W G *et al.* (2004) Carbon exchange and venting anomalies in an upland deciduous forest in northern Wisconsin, USA. *Agricultural and Forest Meteorology,* **126**, 271-295.

Cox P M, Betts R A, Jones C D, Spall S A, Totterdell I J (2000) Acceleration of global warming due to carbon-cycle feedbacks in a coupled climate model. *Nature,* **408**, 184-187.

Craine J, Wedin D, Chapin F (1999) Predominance of ecophysiological controls on soil CO2 flux in a Minnesota grassland. *Plant and Soil,* **207**, 77-86.

Curiel-Yuste J, Janssens I A, Carrara A, Ceulemans R (2004) Annual Q_{10} of soil respiration reflects plant phenological patterns as well as temperature sensitivity. *Global Change Biology,* **10**, 161-169.

Davidson E A, Janssens I A, Luo Y (2006a) On the variability of respiration in terrestrial ecosystems: moving beyond Q10. *Global Change Biology,* **12**, 154-164.

Davidson E A, Richardson A D, Savage K E and Hollinger D.Y. (2006b). A distinct seasonal pattern of the ratio of soil respiration to total ecosystem respiration in a spruce-dominated forest. Global Change Biology, 12: 230-239.

Davidson EA, Belk E, Boone RD (1998) Soil water content and temperature as independent or confounded factors controlling soil respiration in a temperate mixed hardwood forest. Global Change Biology, 4, 217–227.

Davis K J, Bakwin P S, Yi C X, Berger B W, Zhao C L, Teclaw R M, Isebrands J G (2003) The annual cycles of CO2 and H2O exchange over a northern mixed forest as observed from a very tall tower. *Global Change Biology,* **9**, 1278-1293.

De Vries W, Solberg S, Dobbertin M *et al.* (2008) Ecologically implausible carbon response? *Nature,* **451**, E1-E3.

Deforest J, Noormets A, Mcnulty S, Sun G, Tenney G, Chen J (2006) Phenophases alter the soil respiration–temperature relationship in an oak-dominated forest. *International Journal of Biometeorology,* **51**, 135-144.

Del Grosso S J, Parton W J, Mosier a R, Holland E A, Pendall E, Schimel D S, Ojima D S (2005) Modeling soil CO2 emissions from ecosystems. *Biogeochemistry,* **73**, 71-91.

Desai a R, Bolstad P V, Cook B D, Davis K J, Carey E V (2005) Comparing net ecosystem exchange of carbon dioxide between an old-growth and mature forest in the upper Midwest, USA. *Agricultural and Forest Meteorology,* **128**, 33-55.

Dolman a J, Moors E J, Elbers J A (2002) The carbon uptake of a mid latitude pine forest growing on sandy soil. *Agricultural and Forest Meteorology,* **111**, 157-170.

Dore S, Kolb T E, Montes-Helu M *et al.* (2008) Long-term impact of a stand-replacing fire on ecosystem CO2 exchange of a ponderosa pine forest. *Global Change Biology,* **14**, 1801-1820.

Efron B, Tibshirani R (1993) *An Introduction to the Bootstrap,* New York.

Falge E, Baldocchi D, Olson R *et al.* (2001) Gap filling strategies for defensible annual sums of net ecosystem exchange. *Agricultural and Forest Meteorology,* **107**, 43-69.

Fischer M L, Billesbach D P, Berry J A, Riley W J, Torn M S (2007) Spatiotemporal variations in growing season exchanges of CO2, H2O, and sensible heat in agricultural fields of the Southern Great Plains. *Earth Interactions,* **11**.

Flanagan L B, Wever L A, Carlson P J (2002) Seasonal and interannual variation in carbon dioxide exchange and carbon balance in a northern temperate grassland. *Global Change Biology,* **8**, 599-615.

Freeman C, Fenner N, Ostle N J *et al.* (2004) Export of dissolved organic carbon from peatlands under elevated carbon dioxide levels. *Nature,* **430**, 195-198.

Galloway J N, Townsend a R, Erisman J W *et al.* (2008) Transformation of the nitrogen cycle: Recent trends, questions, and potential solutions. *Science,* **320**, 889-892.

Garbulsky M F, Penuelas J, Papale D, Filella I (2008) Remote estimation of carbon dioxide uptake by a Mediterranean forest. *Global Change Biology,* **14**, 2860-2867.

Gaumont-Guay D, Black T A, Barr a G, Jassal R S, Nesic Z (2008) Biophysical controls on rhizospheric and heterotrophic components of soil respiration in a boreal black spruce stand. *Tree Physiology,* **28**, 161-171.

Gibbons, JD and Chakraborti S (2003) *Nonparametric Statistical Inference*, 4th Edition, Marcel Dekker, New York.

Gilmanov T G, Soussana J E, Aires L *et al.* (2007) Partitioning European grassland net ecosystem CO2 exchange into gross primary productivity and ecosystem respiration using light response function analysis. *Agriculture Ecosystems & Environment,* **121**, 93-120.

Gilmanov T G, Tieszen L L, Wylie B K *et al.* (2005) Integration of CO2 flux and remotely-sensed data for primary production and ecosystem respiration analyses in the Northern Great Plains: potential for quantitative spatial extrapolation. *Global Ecology and Biogeography,* **14**, 271-292.

Gough C M, Vogel C S, Schmid H P, Su H B, Curtis P S (2008) Multi-year convergence of biometric and meteorological estimates of forest carbon storage. *Agricultural and Forest Meteorology,* **148**, 158-170.

Goulden M L, Winston G C, Mcmillan a M S, Litvak M E, Read E L, Rocha a V, Elliot J R (2006) An eddy covariance mesonet to measure the effect of forest age on land-atmosphere exchange. *Global Change Biology,* **12**, 2146-2162.

Granier A, Ceschia E, Damesin C *et al.* (2000) The carbon balance of a young Beech forest. *Functional Ecology,* **14**, 312-325.

Grant R F, Oechel W C, Ping C L (2003) Modelling carbon balances of coastal arctic tundra under changing climate. *Global Change Biology,* **9**, 16-36.

Grunwald T, Bernhofer C (2007) A decade of carbon, water and energy flux measurements of an old spruce forest at the Anchor Station Tharandt. *Tellus Series B-Chemical and Physical Meteorology,* **59**, 387-396.

Grunzweig J M, Lin T, Rotenberg E, Schwartz A, Yakir D (2003) Carbon sequestration in arid-land forest. *Global Change Biology,* **9**, 791-799.

Gu F X, Cao M K, Wen X F, Liu Y F, Tao B (2006) A comparison between simulated and measured CO2 and water flux in a subtropical coniferous forest. *Science in China Series D-Earth Sciences,* **49**, 241-251.

Hanson P J, Amthor J S, Wullschleger S D *et al.* (2004) Oak forest carbon and water simulations: Model intercomparisons and evaluations against independent data. *Ecological Monographs,* **74**, 443-489.

Hattenschwiler S, Vitousek P M (2000) The role of polyphenols in terrestrial ecosystem nutrient cycling. *Trends in Ecology & Evolution,* 15, 238-243.

Hibbard K A, Law B E, Reichstein M, Sulzman J (2005) An analysis of soil respiration across northern hemisphere temperate ecosystems. *Biogeochemistry,* **73**, 29-70.

Hirano T, Segah H, Harada T, Limin S, June T, Hirata R, Osaki M (2007) Carbon dioxide balance of a tropical peat swamp forest in Kalimantan, Indonesia. *Global Change Biology,* **13**, 412-425.

Hogberg P, Nordgren A, Buchmann N *et al.* (2001) Large-scale forest girdling shows that current photosynthesis drives soil respiration. *Nature,* **411**, 789-792.

Hollinger D Y, Aber J, Dail B *et al.* (2004) Spatial and temporal variability in forest-atmosphere CO2 exchange. *Global Change Biology,* **10**, 1689-1706.

Houborg R M, Soegaard H (2004) Regional simulation of ecosystem CO2 and water vapor exchange for agricultural land using NOAA AVHRR and Terra MODIS satellite data. Application to Zealand, Denmark. *Remote Sensing of Environment,* **93**, 150-167.

Houghton R A, Davidson E A, Woodwell G M (1998) Missing sinks, feedbacks, and understanding the role of terrestrial ecosystems in the global carbon balance. *Global Biogeochemical Cycles,* **12**, 25-34.

Humphreys E R, Black T A, Morgenstern K, Cai T B, Drewitt G B, Nesic Z, Trofymow J A (2006) Carbon dioxide fluxes in coastal Douglas-fir stands at different stages of development after clearcut harvesting. *Agricultural and Forest Meteorology,* **140**, 6-22.

Hungate B A, Reichstein M, Dijkstra P *et al.* (2002) Evapotranspiration and soil water content in a scrub-oak woodland under carbon dioxide enrichment. *Global Change Biology,* **8**, 289-298.

Irvine J, Law B E, Kurpius M R (2005) Coupling of canopy gas exchange with root and rhizosphere respiration in a semi-arid forest. *Biogeochemistry,* **73**, 271-282.

Janssen P H M, Heuberger P S C (1995) Calibration of Process-Oriented Models. *Ecological Modelling,* **83**, 55-66.

Janssens I A, Lankreijer H, Matteucci G *et al.* (2001) Productivity overshadows temperature in determining soil and ecosystem respiration across European forests. *Global Change Biology,* **7**, 269-278.

Janssens I A, Pilegaard K (2003) Large seasonal changes in Q10 of soil respiration in a beech forest. *Global Change Biology,* **9**, 911-918.

Jenkins J P, Richardson a D, Braswell B H, Ollinger S V, Hollinger D Y, Smith M L (2007) Refining light-use efficiency calculations for a deciduous forest canopy using simultaneous tower-based carbon flux and radiometric measurements. *Agricultural and Forest Meteorology,* **143**, 64-79.

Jenkinson D S, Adams D E, Wild A (1991) Model Estimates of Co2 Emissions from Soil in Response to Global Warming. *Nature,* **351**, 304-306.

Jolly W M, Nemani R, Running S W (2005) A generalized, bioclimatic index to predict foliar phenology in response to climate. *Global Change Biology,* **11**, 619-632.

Kato T, Tang Y H, Gu S, Hirota M, Du M Y, Li Y N, Zhao X Q (2006) Temperature and biomass influences on interannual changes in CO2 exchange in an alpine meadow on the Qinghai-Tibetan Plateau. *Global Change Biology,* **12**, 1285-1298.

Kljun N, Black T A, Griffis T J *et al.* (2006) Response of net ecosystem productivity of three boreal forest stands to drought. *Ecosystems,* **9**, 1128-1144.

Knohl A, Buchmann N (2005) Partitioning the net CO2 flux of a deciduous forest into respiration and assimilation using stable carbon isotopes. *Global Biogeochemical Cycles,* **19**.

Knohl A, Schulze E D, Kolle O, Buchmann N (2003) Large carbon uptake by an unmanaged 250-year-old deciduous forest in Central Germany. *Agricultural and Forest Meteorology,* **118**, 151-167.

Knorr M, Frey S D, Curtis P S (2005) Nitrogen additions and litter decomposition: A meta-analysis. *Ecology,* **86**, 3252-3257.

Kuzyakov Y, Cheng W (2001) Photosynthesis controls of rhizosphere respiration and organic matter decomposition. *Soil Biology and Biochemistry,* **33**, 1915-1925.

Lafleur P M, Roulet N T, Bubier J L, Frolking S, Moore T R (2003) Interannual variability in the peatland-atmosphere carbon dioxide exchange at an ombrotrophic bog. *Global Biogeochemical Cycles,* **17**.

Lasslop G, Reichstein M, Detto M, Richardson a D, Baldocchi D D (2009) Comment on Vickers et al.: Self-correlation between assimilation and respiration resulting from flux partitioning of eddy-covariance CO2 fluxes. *Agricultural and Forest Meteorology,* In Press, Corrected Proof.

Lasslop G, Reichstein M, Papale D *et al.*(2010) Separation of net ecosystem exchange into assimilation and respiration using a light response curve approach: critical issues and global evaluation. *Global Change Biology,* 16, 187-208.

Law B E, Thornton P E, Irvine J, Anthoni P M, Van Tuyl S (2001) Carbon storage and fluxes in ponderosa pine forests at different developmental stages. *Global Change Biology,* **7**, 755-777.

Law B E, Williams M, Anthoni P M, Baldocchi D D, Unsworth M H (2000) Measuring and modelling seasonal variation of carbon dioxide and water vapour exchange of a Pinus ponderosa forest subject to soil water deficit. *Global Change Biology,* **6**, 613-630.

Lipson D A, Wilson R F, Oechel W C (2005) Effects of elevated atmospheric CO2 on soil microbial biomass, activity, and diversity in a chaparral ecosystem. *Applied and Environmental Microbiology,* **71**, 8573-8580.

Liu H P, Randerson J T, Lindfors J, Chapin F S (2005) Changes in the surface energy budget after fire in boreal ecosystems of interior Alaska: An annual perspective. *Journal of Geophysical Research-Atmospheres,* **110**.

Liu Q, Edwards N T, Post W M, Gu L, Ledford J, Lenhart S (2006) Free air CO2 enrichment (FACE) ; soil respiration; temperature response. *Global Change Biology,* **12**, 2136-2145.

Lloyd C R (2006) Annual carbon balance of a managed wetland meadow in the Somerset Levels, UK. *Agricultural and Forest Meteorology,* **138**, 168-179.

Lloyd J, Taylor J A (1994) On the temperature dependence of soil respiration. *Functional Ecology*, 315-323.

Ma S, Baldocchi D D, Xu L, Hehn T (2007) Inter-annual variability in carbon dioxide exchange of an oak/grass savanna and open grassland in California. *Agricultural and Forest Meteorology,* **147**, 157-171.

Magnani F, Mencuccini M, Borghetti M *et al.* (2007) The human footprint in the carbon cycle of temperate and boreal forests. *Nature,* **447**, 848-850.

Marcolla B, Cescatti A (2005) Experimental analysis of flux footprint for varying stability conditions in an alpine meadow. *Agricultural and Forest Meteorology,* **135**, 291-301.

Mccaughey J H, Pejam M R, Arain M A, Cameron D A (2006) Carbon dioxide and energy fluxes from a boreal mixedwood forest ecosystem in Ontario, Canada. *Agricultural and Forest Meteorology,* **140**, 79-96.

Mencuccini M, Holtta T (2010) The significance of phloem transport for the speed with which canopy photosynthesis and belowground respiration are linked. *New Phytologist*, 185, 189-203.

Meyers T P, Hollinger S E (2004) An assessment of storage terms in the surface energy balance of maize and soybean. *Agricultural and Forest Meteorology,* **125**, 105-115.

Migliavacca M, Cremonese E, Colombo R *et al.* (2008) European larch phenology in the Alps: can we grasp the role of ecological factors by combining field observations and inverse modelling? *International Journal of Biometeorology,* **52**, 587-605.

Migliavacca M, Meroni M, Manca G *et al.* (2009) Seasonal and interannual patterns of carbon and water fluxes of a poplar plantation under peculiar eco-climatic conditions. *Agricultural and Forest Meteorology,* **149**, 1460-1476.

Monson R K, Turnipseed a A, Sparks J P, Harley P C, Scott-Denton L E, Sparks K, Huxman T E (2002) Carbon sequestration in a high-elevation, subalpine forest. *Global Change Biology,* **8**, 459-478.

Montagnani L, Manca G, Canepa E *et al.* (2009) A new mass conservation approach to the study of CO2advection in an alpine forest. *J. Geophys. Res.,* **114**.

Moureaux C, Debacq A, Bodson B, Heinesch B, Aubinet M (2006) Annual net ecosystem carbon exchange by a sugar beet crop. *Agricultural and Forest Meteorology,* **139**, 25-39.

Moyano F E, Kutsch W L, Rebmann C (2008) Soil respiration fluxes in relation to photosynthetic activity in broad-leaf and needle-leaf forest stands. *Agricultural and Forest Meteorology,* **148**, 135-143.

Moyano F E, Kutsch W L, Schulze E D (2007) Response of mycorrhizal, rhizosphere and soil basal respiration to temperature and photosynthesis in a barley field. *Soil Biology & Biochemistry,* **39**, 843-853.

Nobel P S (2005) *Physicochemical and Environmental Plant Physiology*, Elsevier Academic Press.

Noormets A, Chen J, Crow T (2007) Age-Dependent Changes in Ecosystem Carbon Fluxes in Managed Forests in Northern Wisconsin, USA. *Ecosystems,* **10**, 187-203.

Noormets A, Gavazzi M J, Mcnulty S G, Domec J, Sun G, King J S, Chen J (2009) Response of carbon fluxes to drought in a coastal plain loblolly pine forest. *Global Change Biology*.

Ogee J, Peylin P, Ciais P *et al.* (2003) Partitioning net ecosystem carbon exchange into net assimilation and respiration using (CO2)-C-13 measurements: A cost-effective sampling strategy. *Global Biogeochemical Cycles,* **17**.

Owen K E, Tenhunen J, Reichstein M *et al.* (2007) Linking flux network measurements to continental scale simulations: ecosystem carbon dioxide exchange capacity under non-water-stressed conditions. *Global Change Biology,* **13**, 734-760.

Papale D, Reichstein M, Aubinet M *et al.* (2006) Towards a standardized processing of Net Ecosystem Exchange measured with eddy covariance technique: algorithms and uncertainty estimation. *Biogeosciences,* **3**, 571-583.

Papale D, Valentini A (2003) A new assessment of European forests carbon exchanges by eddy fluxes and artificial neural network spatialization. *Global Change Biology,* **9**, 525-535.

Pastor J, Stillwell M A, Tilman D (1987) Little bluestem litter dynamics in Minnesota old fields. *Oecologia,* 72, 327-330.

Pataki D E, Bowling D R, Ehleringer J R (2003) Seasonal cycle of carbon dioxide and its isotopic composition in an urban atmosphere: Anthropogenic and biogenic effects. *Journal of Geophysical Research-Atmospheres,* **108**.

Peel M C, Finlayson B L, Mcmahon T A (2007) Updated world map of the Köppen-Geiger climate classification. *Hydrol. Earth Syst. Sci.,* **11**, 1633-1644.

Pereira J S, Mateus J A, Aires L M *et al.* (2007) Net ecosystem carbon exchange in three contrasting Mediterranean ecosystems - the effect of drought. *Biogeosciences,* **4**, 791-802.

Persson T, Karlsson P S, Seyferth U, Sjoberg R M, Rudebeck A (2000) *Carbon mineralization in European forest soils,* Berlin, Springer.

Powell T L, Bracho R, Li J H, Dore S, Hinkle C R, Drake B G (2006) Environmental controls over net ecosystem carbon exchange of scrub oak in central Florida. *Agricultural and Forest Meteorology,* **141**, 19-34.

Powell T L, Gholz H L, Kenneth L, Starr C G, Cropper W P, Martin T A (2008) Carbon exchange of a mature, naturally regenerated pine forest in north Florida. *Global Change Biology,* **14**, 2523-2538.

Raich J W, Potter C S, Bhagawati D (2002) Interannual variability in global soil respiration, 1980-94. *Global Change Biology,* **8**, 800-812.

Raich J W, Schlesinger W H (1992) The global carbon dioxide flux in soil respiration and its relationship to vegetation and climate. *Tellus B,* **44**, 81-99.

Rambal S, Ourcival J M, Joffre R, Mouillot F, Nouvellon Y, Reichstein M, Rocheteau A (2003) Drought controls over conductance and assimilation of a Mediterranean evergreen ecosystem: scaling from leaf to canopy. *Global Change Biology,* **9**, 1813-1824.

Rebmann C, Gockede M, Foken T *et al.* (2005) Quality analysis applied on eddy covariance measurements at complex forest sites using footprint modelling. *Theoretical and Applied Climatology,* **80**, 121-141.

Reichstein M, Beer C (2008) Soil respiration across scales: The importance of a model-data integration framework for data interpretation. *Journal of Plant Nutrition and Soil Science,* **171**, 344-354.

Reichstein M, Ciais P, Papale D *et al.* (2007) Reduction of ecosystem productivity and respiration during the European summer 2003 climate anomaly: a joint flux tower, remote sensing and modelling analysis. *Global Change Biology,* **13**, 634-651.

Reichstein M, Falge E, Baldocchi D *et al.* (2005) On the separation of net ecosystem exchange into assimilation and ecosystem respiration: review and improved algorithm. *Global Change Biology,* **11**, 1424-1439.

Reichstein M, Rey A, Freibauer A *et al.* (2003a) Modeling temporal and large-scale spatial variability of soil respiration from soil water availability, temperature and vegetation productivity indices. *Global Biogeochemical Cycles,* **17**.

Reichstein M, Tenhunen J, Roupsard O *et al.* (2003b) Inverse modeling of seasonal drought effects on canopy CO2/H2O exchange in three Mediterranean ecosystems. *Journal of Geophysical Research-Atmospheres,* **108**.

Reichstein M, Tenhunen J D, Roupsard O *et al.* (2002) Severe drought effects on ecosystem CO2 and H2O fluxes at three Mediterranean evergreen sites: revision of current hypotheses? *Global Change Biology,* **8**, 999-1017.

Ricciuto D M, Butler M P, Davis K J, Cook B D, Bakwin P S, Andrews A, Teclaw R M (2008) Causes of interannual variability in ecosystem-atmosphere CO2 exchange in a northern Wisconsin forest using a Bayesian model calibration. *Agricultural and Forest Meteorology,* **148**, 309-327.

Richardson A D, Braswell B H, Hollinger D Y *et al.* (2006) Comparing simple respiration models for eddy flux and dynamic chamber data. *Agricultural and Forest Meteorology,* **141**, 219-234.

Richardson A D, Hollinger D Y (2005) Statistical modeling of ecosystem respiration using eddy covariance data: Maximum likelihood parameter estimation, and Monte Carlo simulation of model and parameter uncertainty, applied to three simple models. *Agricultural and Forest Meteorology,* **131**, 191-208.

Rodeghiero M, Cescatti A (2005) Main determinants of forest soil respiration along an elevation/temperature gradient in the Italian Alps. *Global Change Biology,* **11**, 1024-1041.

Rodhe H, Dentener F, Schulz M (2002) The global distribution of acidifying wet deposition. *Environmental Science & Technology,* **36**, 4382-4388.

Roupsard O, Bonnefond J M, Irvine M *et al.* (2006) Partitioning energy and evapo-transpiration above and below a tropical palm canopy. *Agricultural and Forest Meteorology,* **139**, 252-268.

Santos a J B, Quesada C A, Da Silva G T, Maia J F, Miranda H S, Miranda C, Lloyd J (2004) High rates of net ecosystem carbon assimilation by Brachiara pasture in the Brazilian Cerrado. *Global Change Biology,* **10**, 877-885.

Savage K, Davidson E A, Richardson A D, Hollinger D Y (2009) Three scales of temporal resolution from automated soil respiration measurements. *Agricultural and Forest Meteorology,* **149**, 2012-2021.

Schmid H P, Grimmond C S B, Cropley F, Offerle B, Su H B (2000) Measurements of CO2 and energy fluxes over a mixed hardwood forest in the mid-western United States. *Agricultural and Forest Meteorology,* **103**, 357-374.

Shono H (2005) Is model selection using Akaike's information criterion appropriate for catch per unit effort standardization in large samples? *Fisheries Science,* **71**, 978-986.

Staudt K and Foken T. Documentation of reference data for the experimental areas of the Bayreuth Centre for Ecology and Environmental Research (BayCEER) at the Waldstein site Arbeitsergebnisse, Universität Bayreuth, Abt. Mikrometeorologie, Print, ISSN 1614-8916, 2007, No. 35, 35

Suni T, Berninger F, Vesala T *et al.* (2003a) Air temperature triggers the recovery of evergreen boreal forest photosynthesis in spring. *Global Change Biology,* **9**, 1410-1426.

Suni T, Rinne J, Reissell A *et al.* (2003b) Long-term measurements of surface fluxes above a Scots pine forest in Hyytiala, southern Finland, 1996-2001. *Boreal Environment Research,* **8**, 287-301.

Sutton M A, Simpson D, Levy P E, Smith R I, Reis S, Van Oijen M, De Vries W (2008) Uncertainties in the relationship between atmospheric nitrogen deposition and forest carbon sequestration. *Global Change Biology,* **14**, 2057-2063.

Syed K H, Flanagan L B, Carlson P J, Glenn a J, Van Gaalen K E (2006) Environmental control of net ecosystem CO2 exchange in a treed, moderately rich fen in northern Alberta. *Agricultural and Forest Meteorology,* **140**, 97-114.

Takagi K, Fukuzawa K, Liang N *et al.* (2009) Change in CO2 balance under a series of forestry activities in a cool-temperate mixed forest with dense undergrowth. *Global Change Biology,* **15**, 1275-1288.

Tang J W, Baldocchi D D (2005) Spatial-temporal variation in soil respiration in an oak-grass savanna ecosystem in California and its partitioning into autotrophic and heterotrophic components. *Biogeochemistry,* **73**, 183-207.

Thornton P E, Law B E, Gholz H L *et al.* (2002) Modeling and measuring the effects of disturbance history and climate on carbon and water budgets in evergreen needleleaf forests. *Agricultural and Forest Meteorology,* **113**, 185-222.

Thomas C K, Law B E, Irvine J, Martin J G, Pettijohn J C, and Davis K J, 2009. Seasonal hydrology explains inter-annual and seasonal variation in carbon and water exchange in a semi-arid mature Ponderosa Pine forest in Central Oregon, J. Geophys. Res. Biogeosciences (in press).

Tietema A, Riemer L, Verstraten J M, Vandermaas M P, Vanwijk a J, Vanvoorthuyzen I (1993) Nitrogen cycling in acid forest soils subject to increased atmospheric nitrogen input. *Forest Ecology and Management,* 57, 29-44.

Urbanski S, Barford C, Wofsy S *et al.* (2007) Factors controlling CO2 exchange on timescales from hourly to decadal at Harvard Forest. *Journal of Geophysical Research-Biogeosciences,* **112**, 25.

Valentini R, Matteucci G, Dolman a J *et al.* (2000) Respiration as the main determinant of carbon balance in European forests. *Nature,* **404**, 861-865.

Van Der Molen M K, Van Huissteden J, Parmentier F J W *et al.* (2007) The growing season greenhouse gas balance of a continental tundra site in the Indigirka lowlands, NE Siberia. *Biogeosciences,* **4**, 985-1003.

Veenendaal E M, Kolle O, Lloyd J (2004) Seasonal variation in energy fluxes and carbon dioxide exchange for a broad-leaved semi-arid savanna (Mopane woodland) in Southern Africa. *Global Change Biology,* **10**, 318-328.

Venables W N, Ripley B D (2002) *Modern Applied Statistics with S,* New York, Springer.

Verbeeck H, Samson R, Verdonck F, Lemeur R (2006) Parameter sensitivity and uncertainty of the forest carbon flux model FORUG: a Monte Carlo analysis. *Tree Physiology,* **26**, 807-817.

Verma S B, Dobermann A, Cassman K G *et al.* (2005) Annual carbon dioxide exchange in irrigated and rainfed maize-based agroecosystems. *Agricultural and Forest Meteorology,* **131**, 77-96.

Veroustraete F, Sabbe H, Eerens H (2002) Estimation of carbon mass fluxes over Europe using the C-Fix model and Euroflux data. *Remote Sensing of Environment,* 83, 376-399.

Vickers D, Thomas C K, Martin J G, Law B (2009) Self-correlation between assimilation and respiration resulting from flux partitioning of eddy-covariance CO2 fluxes. *Agricultural and Forest Meteorology,* **149**, 1552-1555.

Vitousek P M, Hobbie S (2000) Heterotrophic nitrogen fixation in decomposing litter: Patterns and regulation. *Ecology,* 81, 2366-2376.

Wohlfahrt G, Anderson-Dunn M, Bahn M *et al.* (2008a) Biotic, Abiotic, and Management Controls on the Net Ecosystem CO2 Exchange of European Mountain Grassland Ecosystems. *Ecosystems,* **11**, 1338-1351.

Wohlfahrt G, Anfang C, Bahn M *et al.* (2005a) Quantifying nighttime ecosystem respiration of a meadow using eddy covariance, chambers and modelling. *Agricultural and Forest Meteorology,* **128**, 141-162.

Wohlfahrt G, Bahn M, Haslwanter A, Newesely C, Cernusca A (2005b) Estimation of daytime ecosystem respiration to determine gross primary production of a mountain meadow. *Agricultural and Forest Meteorology,* **130**, 13-25.

Wohlfahrt G, Hammerle A, Haslwanter A, Bahn M, Tappeiner U, Cernusca A (2008b) Seasonal and inter-annual variability of the net ecosystem CO2 exchange of a temperate mountain grassland: Effects of weather and management. *J. Geophys. Res.,* **113**.

Xu L K, Baldocchi D D (2004) Seasonal variation in carbon dioxide exchange over a Mediterranean annual grassland in California. *Agricultural and Forest Meteorology,* **123**, 79-96.

Yamashita T, Yamashita K, Kamimura R (2007) A stepwise AIC method for variable selection in linear regression. *Communications in Statistics-Theory and Methods,* **36**, 2395-2403.

Yi C X, Li R Z, Bakwin P S *et al.* (2004) A nonparametric method for separating photosynthesis and respiration components in CO2 flux measurements. *Geophysical Research Letters,* **3**

Table 1 - Different model formulation of the dependency of ecosystem respiration (R_{ECO}) on Gross Primary Productivity (GPP) used in this analysis.

Model	Formula
LinGPP	$R_{ECO} = (R_0 + k_2 GPP) \cdot e^{E_0\left(\frac{1}{T_{ref}-T_0}-\frac{1}{T_A-T_0}\right)} \cdot \frac{\alpha k + P(1-\alpha)}{k + P(1-\alpha)}$
ExpGPP	$R_{ECO} = \left[R_0 + R_2\left(1 - e^{k_2 GPP}\right)\right] \cdot e^{E_0\left(\frac{1}{T_{ref}-T_0}-\frac{1}{T_A-T_0}\right)} \cdot \frac{\alpha k + P(1-\alpha)}{k + P(1-\alpha)}$
MicMenGPP	$R_{ECO} = \left[R_0 + \frac{R_{MAX} GPP}{GPP + hR_{MAX}}\right] \cdot e^{E_0\left(\frac{1}{T_{ref}-T_0}-\frac{1}{T_A-T_0}\right)} \cdot \frac{\alpha k + P(1-\alpha)}{k + P(1-\alpha)}$
addLinGPP	$R_{ECO} = R_0 \cdot e^{E_0\left(\frac{1}{T_{ref}-T_0}-\frac{1}{T_A-T_0}\right)} \cdot \frac{\alpha k + P(1-\alpha)}{k + P(1-\alpha)} + k_2 GPP$
addExpGPP	$R_{ECO} = R_0 \cdot e^{E_0\left(\frac{1}{T_{ref}-T_0}-\frac{1}{T_A-T_0}\right)} \cdot \frac{\alpha k + P(1-\alpha)}{k + P(1-\alpha)} + R_2\left(1 - e^{k_2 GPP}\right)$
addMicMenGPP	$R_{ECO} = R_0 \cdot e^{E_0\left(\frac{1}{T_{ref}-T_0}-\frac{1}{T_A-T_0}\right)} \cdot \frac{\alpha k + P(1-\alpha)}{k + P(1-\alpha)} + \frac{R_{MAX} GPP}{GPP + hR_{MAX}}$

Table 2 - Statistics of fit for the climate-driven model (*'TP Model'*) and the best model selected among the models listed in Tab. 1 according to the consistent Akaike Information Criterion (cAIC). Statistics are averaged per Plant Functional Type (PFT). Except for croplands (CRO), 'LinGPP' is selected as the best model formulation. EF is the modelling efficiency while RMSE is the root mean square error (Jannsens and Heuberger, 1995). The definitions of different PFTs are: evergreen needleleaf forest (ENF), deciduous broadleaf forest (DBF), grasslands (GRA), croplands (CRO), savannah (SAV), shrublands (SHB), evergreen broadleaf forest (EBF), mixed forest (MF), wetland (WET). The list of acronyms is also provided in Appendix II. Values in brackets are the standard deviations.

	'TP Model'		*'LinGPP Model'*		**Best Model Selected**
PFT	**EF**	**RMSE**	**EF**	**RMSE**	
ENF	0.71(0.14)	1.02 (0.35)	0.78 (0.14)	0.83 (0.21)	*LinGPP*
DBF	0.63 (0.17)	1.15 (0.51)	0.72 (0.13)	0.98 (0.41)	*LinGPP*
GRA	0.62 (0.18)	1.35 (0.43)	0.83 (0.07)	0.91 (0.33)	*LinGPP*
CRO	0.55 (0.18)	1.55 (0.53)	0.82 (0.08)	1.01 (0.33)	*addLinGPP*
SAV	0.38 (0.16)	0.78 (0.24)	0.72 (0.06)	0.53 (0.15)	*LinGPP*
SHB	0.59 (0.29)	0.67 (0.50)	0.66 (0.29)	0.58 (0.51)	*LinGPP*
EBF	0.42 (0.27)	1.11 (0.55)	0.58 (0.23)	0.91 (0.49)	*LinGPP*
MF	0.67 (0.18)	0.96 (0.72)	0.82 (0.13)	0.78 (0.50)	*LinGPP*
WET	0.67 (0.18)	0.96 (0.51)	0.85 (0.48)	0.79 (0.07)	*LinGPP*

Table 3 – Results of the model selection conducted with the Stepwise AIC method for the sites belonging to all the PFT (*All PFTs*) and for undisturbed temperate and boreal forests identified in the Appendix II (*Undisturbed Forests*). Coefficients (a_1,a_2, const), their significance and the statistics of the best model selected are reported. In parenthesis the standard error of the coefficients are reported. The significance of coefficients is also reported (* p<0.001, ** p<0.01, * p<0.05, . p<0.1).**

Model	Best Model Selected	a_1		a_2		const		r^2	r^2 adj.	*p*	n
All PFTs	R_0=$a_1 LAI_{MAX}$+a_2 *SoilC* + *const*	0.412	***	0.045	**	*0.582*	*	0.58	0.57	<0.001	68
		(0.048)		(0.015)		*(0.251)*					
Undisturbed Forest (MF+DBF+ENF)	R_0= $a_1 LAI_{MAX}$ + a_2 N_{depo} + *const*	0.469	***	-0.025	.	0.948	*	0.70	0.67	<0.001	23
		(0.069)		(0.017)		(0.377)					
Disturbed Forests	R_0= a_1*SoilC* + a_2 T_{MEAN} + *const*	0.211	**	-0.188	**	3.487	*	0.85	0.80	<0.001	10
		(0.051)		(0.059)		(0.982)					

Table 4 – Parameters of the relationships between reference respiration (R_0) defined at 15°C and seasonal maximum LAI for each Plant Functional Type (PFT). The standard errors of model parameters are reported in parenthesis. Determination coefficients and statistical significance are also shown.– *'TPGPP-LAI Model'* parameters estimated for each Plant Functional Type (see Appendix II). Standard errors estimated with the bootstrap algorithm are reported in parentheses. Model statistics are also given. *''TPGPP-LAI Model'* is defined in Eq. 9. The definitions of different PFTs are: evergreen needleleaf forest (ENF), deciduous broadleaf forest (DBF), grasslands (GRA), croplands (CRO), savannah (SAV), shrublands (SHB), evergreen broadleaf forest (EBF), mixed forest (MF), wetland (WET).

PFT	Parameters and statistics (R0 vs LAI_{MAX})				Final Model Parameters				Fitting statistics			
	$R_{LAI=0}$	a_{LAI}	r^2	*p*	k_2	E_0 [K]	A	K [mm]	r^2	EF	RMSE [$gCm^{-2}day^{-1}$]	MAE [$gCm^{-2}day^{-1}$]
ENF	1.02 (0.42)	0.42 (0.08)	0.50	*<0.001*	0.478 (0.013)	124.833 (4.656)	0.604 (0.065)	0.222 (0.070)	0.79	0.70	1.072	0.788
DBF	1.27 (0.50)	0.34 (0.10)	0.46	*<0.01*	0.247 (0.009)	87.655 (4.405)	0.796 (0.031)	0.184 (0.064)	0.65	0.52	1.322	0.899
GRA	0.41 (0.71)	1.14 (0.33)	0.60	*<0.001*	0.578 (0.062)	101.181 (6.362)	0.670 (0.052)	0.765 (1.589)	0.82	0.80	1.083	0.838
CRO	0.25 (0.66)	0.40 (0.11)	0.52	*<0.001*	0.244 (0.016)	129.498 (5.618)	0.934 (0.065)	0.035 (3.018)	0.80	0.79	0.933	0.659
SAV	0.42 (0.39)	0.57 (0.17)	0.54	*<0.005*	0.654 (0.024)	81.537 (7.030)	0.474 (0.018)	0.567 (0.119)	0.65	0.60	0.757	0.535
SHB	0.42 (0.39)	0.57 (0.17)	0.54	*<0.005*	0.354 (0.021)	156.746 (8.222)	0.850 (0.070)	0.097 (1.304)	0.73	0.60	0.618	0.464
EBF	-0.47 (0.50)	0.82 (0.13)	0.87	*<0.001*	0.602 (0.044)	52.753 (4.351)	0.593 (0.032)	2.019 (1.052)	0.55	0.41	1.002	0.792
MF	0.78 (0.18)	0.44 (0.04)	0.52	*<0.001*	0.391 (0.068)	176.542 (8.222)	0.703 (0.083)	2.831 (4.847)	0.86	0.79	0.988	0.723
WET	0.78 (0.18)	0.44 (0.04)	0.52	*<0.001*	0.398 (0.013)	144.705 (8.762)	0.582 (0.163)	0.054 (0.593)	0.87	0.86	0.403	0.292

Table 5 –Statistics of the modelled (x- axis) vs measured (y-axis) annual R_{ECO} with the *'TPGPP-LAI Model'*. Number of site-years for each PFT are also reported. The definitions of different PFTs are: evergreen needleleaf forest (ENF), deciduous broadleaf forest (DBF), grasslands (GRA), croplands (CRO), savannah (SAV), shrublands (SHB), evergreen broadleaf forest (EBF), mixed forest (MF), wetland (WET).

PFT	Statistics						
	r^2	EF	RMSE [gC m^{-2} yr^{-1}]	MAE [gC m^{-2} yr^{-1}]	Slope	Intercept	Site years
ENF	0.76	0.76	210.12	158.00	0.99	30.03	153
DBF	0.40	0.33	175.15	145.44	0.71	263.98	81
GRA	0.89	0.89	153.03	129.16	0.94	36.94	45
CRO	0.74	0.73	131.75	109.54	1.07	-47.68	35
SAV	0.86	0.81	98.80	75.95	1.27	-100.68	18
SHB	0.96	0.95	74.74	71.09	0.95	35.56	17
EBF	0.95	0.95	128.30	100.27	0.98	44.79	28
MF	0.68	0.64	131.44	40.72	0.84	125.90	30
WET	0.97	0.94	13.893	11.88	0.86	21.70	6
All	0.81	0.77	172.79	132.99	0.82	145.51	413

Table 6 – Results of Training/Evaluation splitting and k-fold cross-validation of the *'TPGPP-LAI Model'* averaged per plant functional type as defined in the Appendix II. The definitions of different PFTs are: evergreen needleleaf forest (ENF), deciduous broadleaf forest (DBF), grasslands (GRA), croplands (CRO), savannah (SAV), shrublands (SHB), evergreen broadleaf forest (EBF), mixed forest (MF), wetland (WET).

PFT	Training/Evaluation Splitting				k-fold Cross-Validation			
	r^2	EF	RMSE [$gCm^{-2}day^{-1}$]	MAE [$gCm^{-2}day^{-1}$]	r^2	EF	RMSE [$gCm^{-2}day^{-1}$]	MAE [$gCm^{-2}day^{-1}$]
ENF	0.74	0.74	1.170	0.854	0.76	0.76	1.145	0.827
DBF	0.54	0.48	1.443	1.017	0.58	0.50	1.374	0.967
GRA	0.79	0.79	1.227	0.881	0.81	0.80	1.174	0.819
CRO	0.80	0.80	1.208	0.889	0.80	0.79	1.254	0.926
SAV	0.57	0.54	0.831	0.623	0.60	0.59	0.717	0.515
SHB	0.71	0.58	0.954	0.720	0.68	0.67	1.180	0.790
EBF	0.52	0.28	1.350	0.985	0.70	0.69	0.957	0.928
MF	0.71	0.71	1.326	0.927	0.75	0.74	1.254	0.871
WET	0.79	0.75	0.566	0.320	0.83	0.82	0.490	0.312

Figure Captions

Figure 1 - a) Pearson's correlation coefficients (*r*) for the residual of observed minus modelled R_{ECO} versus measured GPP and a function of time lag; b) average model performances (EF and RMSE) for deciduous broadleaf forests as a function of the time lag between GPP and R_{ECO} response. Results obtained running the 'LinGPP' formulation with different GPP time series, from the GPP measured at the same day up to the GPP measured one week before the R_{ECO}. Error bars represent the standard deviation of model statistics calculated at each site. The definitions of different PFTs are: evergreen needleleaf forest (ENF), deciduous broadleaf forest (DBF), grasslands (GRA), croplands (CRO), savannah (SAV), shrublands (SHB), evergreen broadleaf forest (EBF), mixed forest (MF), wetland (WET).

Figure 2 - Correlation between reference respiration (R_0) and a) seasonal maximum leaf area index (LAI_{MAX}) of understorey and overstorey, b) overstorey peak leaf area index ($LAI_{MAX,o}$), c) total soil carbon content (SoilC), d) stand age for forest ecosystems (Age), e) total atmospheric nitrogen deposition for forest sites (N_{depo}) and f) mean annual temperature. In panels a), b), c), d) and f) different symbols represent different PFT. In panel e) full circles represent disturbed sites while open circles the undisturbed ones. The r^2, *p* and number of sites (n) were reported. The regression line and the 95% confidence interval are given if the relationship is significant. The definitions of different PFTs are: evergreen needleleaf forest (ENF), deciduous broadleaf forest (DBF), grasslands (GRA), croplands (CRO), savannah (SAV), shrublands (SHB), evergreen broadleaf forest (EBF), mixed forest (MF), wetland (WET).

Figure 3 – Scatterplots of annual observed vs modelled R_{ECO} obtained using the *'TPGPP-LAI Model'*. Each panel represent a different plant functional type (PFT). The definitions of different PFTs are: evergreen needleleaf forest (ENF), deciduous broadleaf forest (DBF), grasslands (GRA), croplands (CRO), savannah (SAV), shrublands (SHB), evergreen broadleaf forest (EBF), mixed forest (MF), wetland (WET).

Figure 4 - Time series of average monthly model residuals for different deciduous broadleaf forest (DBF) sites. The vertical grey dashed lines represent the phenological dates. Average phenological dates were derived for US-Ha1 from literature (Jolly et al. 2005) while for other sites they were retrieved from the FLUXNET database. Average phenological dates, bud-burst and end-of-growing season are respectively: US-Ha1 (115-296),DE-Hai (126-288), FR-Hes (120-290), FR-Fon (125-292), IT-Ro1 (104-298) and CA-Oas (146-258)..

Figure 5 – Time series of observed (open circles) and modeled (black circles) for the IT-MBo site (a,b) and for the ES-ES2 site (c, d), grey dashed lines represent the dates of cuts indicated in the database (the date may be indicative), the model underestimation of fluxes in the days after each cut is clear.

Figure 6 – Response function of ecosystem respiration to the 30-day running average of daily precipitation (Eq. 2) for each plant functional type (PFT). The parameters in Table 3 were used to draw the curves. The definitions of different PFTs are: evergreen needleleaf forest (ENF), deciduous broadleaf forest (DBF), grasslands (GRA), croplands (CRO), savannah (SAV), shrublands (SHB), evergreen broadleaf forest (EBF), mixed forest (MF), wetland (WET).

Figure AI – Box-plot of the differences at each site between the Pearson's correlation coefficient between 'TP Model' residuals and GPP computed using FLUXNET partitioning ($r_{TPModel\text{-}GPPFLUX}$) and Lasslop's partitioning ($r_{TPModel\text{-}GPPLasslop}$). Data were grouped in box-plots for each PFT. The definitions of different PFTs are: evergreen needleleaf forest (ENF), deciduous broadleaf forest (DBF), grasslands (GRA), croplands (CRO), savannah (SAV), shrublands (SHB), evergreen broadleaf forest (EBF), mixed forest (MF), wetland (WET)

Figure AII – Box-plot of the parameters a) R_0, b) k_2, c) EF and d) RMSE estimated using FLUXNET (red boxes) and Lasslop's (Blue boxes) partitioning. The median of the differences of parameters governing the response to GPP (k_2) estimated at each site with the two different data-sets are not statistically different from 0 except for ENF and DBF (for both $p<0.05$). No statistical differences were found for model statistics. Data were grouped in box-plots for each PFT. The definitions of different PFTs are: evergreen needleleaf forest (ENF), deciduous broadleaf forest (DBF), grasslands (GRA), croplands (CRO), savannah (SAV), shrublands (SHB), evergreen broadleaf forest (EBF), mixed forest (MF), wetland (WET).

Appendix List

APPENDIX I – Site Table. ID, Name, country, belonging network, coordinates PFT, climate and LAI_{MAX} of the sites used in the analysis. Climate abbreviations follow the Koeppen classification (Peel et al., 2007). Networks are described in www.fluxdata.org

APPENDIX II – Site characteristics derived from the FLUXNET database. R_0 is the reference respiration estimated with the *LinGPP* model formulation, LAI is the maximum seasonal leaf area index of the ecosystems (understorey and overstorey), $LAI_{MAX,o}$ is the maximum leaf area index of the solely overstorey, SoilC is the total soil carbon content, Age is the stand age, T_{mean} is the annual average mean temperature, Ndepo is the total atmospheric nitrogen deposition derived as described in the method section. Sites with (*) in the column dist (disturbance) represent sites with recent disturbance according to what reported in the FLUXNET database.

APPENDIX III – Acronyms and abbreviations.

APPENDIX IV – Discussion of the 'spurious' correlation between R_{ECO} and GPP.

APPENDIX I – Site table

Table AI – Site Table. ID, Name, country, belonging network, coordinates PFT, climate and LAI_{MAX} of the sites used in the analysis. Climate abbreviations follow the Koeppen classification (Peel et al., 2007). Networks are described in www.fluxdata.org. The definitions of different PFTs are: evergreen needleleaf forest (ENF), deciduous broadleaf forest (DBF), grasslands (GRA), croplands (CRO), savannah (SAV), shrublands (SHB), evergreen broadleaf forest (EBF), mixed forest (MF), wetland (WET).

SITE ID	*Tower Name*	*Country*	*Latitude*	*Longitude*	*PFT*	*Climate*	*Reference*
AT-Neu	Neustift/Stubai Valley	Austria	47.12	11.32	GRA	Cfb	(Wohlfahrt *et al.*, 2008b)
AU-How	Howard Springs	Australia	-12.49	131.15	WSA	Aw	(Beringer *et al.*, 2007)
BE-Lon	Lonzee	Belgium	50.55	4.74	CRO	Cfb	(Moureaux et al., 2006)
BE-Vie	Vielsalm	Belgium	50.31	5.99	MF	Cfb	(Aubinet *et al.*, 2001)
BR-Sp1	Sao Paulo Cerrado	Brazil	-21.62	-47.65	WSA	Aw	(Santos et al., 2004)
BW-Ma1	Maun- Mopane Woodland	Botswana	-19.92	23.56	WSA	BSh	(Veenendaal et al., 2004)
CA-Ca1	British Columbia- Campbell River - Mature Forest Site	Canada	49.87	-125.33	ENF	Cfb	(Humphreys et al., 2006)
CA-Ca3	British Columbia- Campbell River - Young Plantation Site	Canada	49.53	-124.90	ENF	Cfb	(Humphreys et al., 2006)
CA-Gro	Ontario- Groundhog River-Mat. Boreal Mixed Wood	Canada	48.22	-82.16	MF	Dfb	(Mccaughey *et al.*, 2006)
CA-Let	Lethbridge	Canada	49.71	-112.94	GRA	Dfb	(Flanagan et al., 2002)
CA-Mer	Eastern Peatland- Mer Bleue	Canada	45.41	-75.52	WET	Dfb	(Lafleur *et al.*, 2003)
CA-NS1	UCI-1850 burn site	Canada	55.88	-98.48	ENF	Dfc	(Goulden et al., 2006)
CA-NS3	UCI-1964 burn site	Canada	55.91	-98.38	ENF	Dfc	(Goulden et al., 2006)
CA-NS6	UCI-1989 burn site	Canada	55.92	-98.96	OSH	Dfc	(Goulden et al., 2006)
CA-Oas	Sask.- SSA Old Aspen	Canada	53.63	-106.20	DBF	Dfc	(Black et al., 2000)
CA-Ojp	Sask.- SSA Old Jack Pine	Canada	53.92	-104.69	ENF	Dfc	(Kljun *et al.*, 2006)
CA-Qfo	Quebec Mature Boreal Forest Site	Canada	49.69	-74.34	ENF	Dfc	(Bergeron *et al.*, 2007)
CA-TP4	Ontario- Turkey Point Mature White Pine	Canada	42.71	-80.36	ENF	Dfb	(Arain & Restrepo-Coupe, 2005)
CA-WP1	Western Peatland- LaBiche-Black Spruce/Larch Fen	Canada	54.95	-112.47	MF	Dfc	(Syed *et al.*, 2006)
CH-Oe1	Oensingen1 grass	Switzerland	47.29	7.73	GRA	Cfb	(Ammann et al., 2007)
CN-HaM	Haibei Alpine Tibet site	China	37.37	101.18	GRA	ET	(Kato *et al.*, 2006)
CN-Ku1	Kubuqi_populus forest	China	40.54	108.69	EBF	BSk	-
CN-Ku2	Kubuqi_shrubland	China	40.38	108.55	OSH	BSk	-
CN-Xi2	Xilinhot grassland site (X03)	China	43.55	116.67	GRA	Dwb	-
DE-Bay	Bayreuth-Waldstein/WeidenBrunnen	Germany	50.14	11.87	ENF	Cfb	(Staudt and Foken 2007)
DE-Hai	Hainich	Germany	51.08	10.45	DBF	Cfb	(Knohl et al., 2003)
DE-Kli	Klingenberg	Germany	50.89	13.52	CRO	Cfb	-
DE-Tha	Tharandt- Anchor Station	Germany	50.96	13.57	ENF	Cfb	(Grunwald & Bernhofer, 2007)
DK-Ris	Risbyholm	Denmark	55.53	12.10	CRO	Cfb	(Houborg & Soegaard, 2004)
ES-ES1	El Saler	Spain	39.35	-0.32	ENF	Csa	(Reichstein et al., 2005)
ES-ES2	El Saler-Sueca	Spain	39.28	-0.32	CRO	Csa	Carrara A. (P.C.)
ES-LMa	Las Majadas del Tietar	Spain	39.94	-5.77	SAV	Csa	-
ES-VDA	Vall d'Alinya	Spain	42.15	1.45	GRA	Cfb	(Gilmanov et al., 2007)

FI-Hyy	Hyytiala	Finland	61.85	24.29	ENF	Dfc	(Suni et al., 2003b)
FI-Sod	Sodankyla	Finland	67.36	26.64	ENF	Dfc	(Suni et al., 2003a)
FI-Kaa	Kaamanen wetland	Finland	69.14	27.30	WET	Dfc	(Aurela et al., 2002)
FR-Fon	Fontainebleau	France	48.48	2.78	DBF	Cfb	-
FR-Gri	Grignon (after 6/5/2005)	France	48.84	1.95	CRO	Cfb	(Hibbard et al., 2005)
FR-Hes	Hesse Forest- Sarrebourg	France	48.67	7.06	DBF	Cfb	(Granier et al., 2000)
FR-LBr	Le Bray (after 6/28/1998)	France	44.72	-0.77	ENF	Cfb	(Ogee et al., 2003)
FR-Lq2	Laqueuille extensive	France	45.64	2.74	GRA	Cfb	(Gilmanov et al., 2007)
FR-Pue	Puechabon	France	43.74	3.60	EBF	Csa	(Rambal et al., 2003)
ID-Pag	Palangkaraya	Indonesia	2.35	114.04	EBF	Af	(Hirano et al., 2007)
IL-Yat	Yatir	Israel	31.34	35.05	ENF	BSh	(Grunzweig et al., 2003)
IT-Amp	Amplero (after 6/28/2004)	Italy	41.90	13.61	GRA	Cfa	(Gilmanov et al., 2007)
IT-BCi	Borgo Cioffi	Italy	40.52	14.96	CRO	Csa	(Reichstein et al., 2003a)
IT-Cpz	Castelporziano	Italy	41.71	12.38	EBF	Csa	(Garbulsky *et al.*, 2008)
IT-MBo	Monte Bondone	Italy	46.02	11.05	GRA	Cfb	(Marcolla & Cescatti, 2005)
IT-Noe	Sardinia/Arca di Noè	Italy	40.61	8.15	CSH	Csa	-
IT-Non	Nonantola	Italy	44.69	11.09	DBF	Cfa	(Reichstein et al., 2005)
IT-PT1	Zerbolò-Parco Ticino- Canarazzo	Italy	45.20	9.06	DBF	Cfa	(Migliavacca *et al.*, 2009)
IT-Ren	Renon/Ritten (Bolzano)	Italy	46.59	11.43	ENF	Cfb	(Montagnani *et al.*, 2009)
IT-Ro1	Roccarespampani 1	Italy	42.41	11.93	DBF	Csa	(Reichstein et al., 2003a)
IT-Ro2	Roccarespampani 2	Italy	42.39	11.92	DBF	Csa	(Reichstein et al., 2003a)
IT-SRo	San Rossore	Italy	43.73	10.28	ENF	Csa	(Chiesi et al., 2005)
JP-Tef	Teshio Experimental Forest	Japan	45.06	142.11	MF	Dfb	(Takagi *et al.*, 2009)
NL-Loo	Loobos	Netherlands	52.17	5.74	ENF	Cfb	(Dolman et al., 2002) LAI (Moors, P.C.)
PT-Esp	Espirra	Portugal	38.64	-8.60	EBF	Csa	-
PT-Mi1	Mitra (Evora)	Portugal	38.54	-8.00	SAV	Csa	(Pereira et al., 2007)
RU-Cok	Chokurdakh	Russia	70.62	147.88	OSH	Dfc	(Van Der Molen *et al.*, 2007)
UK-EBu	Easter Bush- Scotland	UK	55.87	-3.21	GRA	Cfb	-
UK-Gri	Griffin- Aberfeldy-Scotland	UK	56.61	-3.80	ENF	Cfc	(Rebmann et al., 2005)
US-ARb	ARM Southern Great Plains burn site- Lamont	USA	35.55	-98.04	GRA	Cfa	-
US-ARM	ARM Southern Great Plains site- Lamont	USA	36.61	-97.49	CRO	Cfa	(Fischer *et al.*, 2007)
US-Aud	Audubon Research Ranch	USA	31.59	-110.51	GRA	BSk	-
US-Bar	Bartlett Experimental Forest	USA	44.06	-71.29	DBF	Dfb	(Jenkins et al., 2007)
US-Bkg	Brookings	USA	44.35	-96.84	GRA	Dfa	(Gilmanov et al., 2005)
US-Bn1	Bonanza Creek, 1920 Burn site near Delta Junction	USA	63.92	-145.38	ENF	Dsc	(Liu et al., 2005)
US-Bn2	Bonanza Creek, 1987 Burn site near Delta Junction	USA	63.92	-145.38	DBF	Dsc	(Liu et al., 2005)
US-Bn3	Bonanza Creek, 1999 Burn site near Delta Junction	USA	63.92	-145.74	OSH	Dsc	(Liu et al., 2005)
US-Bo1	Bondville	USA	40.01	-88.29	CRO	Dfa	(Meyers & Hollinger, 2004)
US-Brw	Alaska – Barrow	USA	71.32	-156.63	WET	ET	(Grant et al., 2003)
US-Dk3	Duke Forest - loblolly pine	USA	35.98	-79.09	MF	Cfa	(Pataki et al., 2003)
US-FPe	Fort Peck	USA	48.31	-105.10	GRA	BSk	-
US-Fwf	Flagstaff – Wildfire	USA	35.45	-111.77	GRA	Csb	(Dore *et al.*, 2008)
US-Ha1	Harvard Forest EMS Tower (HFR1)	USA	42.54	-72.17	DBF	Dfb	(Urbanski *et al.*, 2007)
US-Ho1	Howland Forest (main tower)	USA	45.20	-68.74	ENF	Dfb	(Hollinger et al., 2004)

US-Ho2	Howland Forest (west tower)	USA	45.21	-68.75	MF	Dfb	(Hollinger et al., 2004)
US-IB1	Fermi National Accelerator Laboratory- Batavia (Agricultural site)	USA	41.86	-88.22	CRO	Dfa	(Allison et al., 2005)
US-KS2	Kennedy Space Center (scrub oak)	USA	28.61	-80.67	CSH	Cfa	(Powell et al., 2006)
US-Los	Lost Creek	USA	46.08	-89.98	CSH	Dfb	(Yi *et al.*, 2004)
US-LPH	Little Prospect Hill	USA	42.54	-72.18	DBF	Dfb	(Borken *et al.*, 2006)
US-Me2	Metolius-intermediate aged ponderosa pine	USA	44.45	-121.56	ENF	Csb	(Thomas et al., in press)
US-Me3	Metolius-second young aged pine	USA	44.32	-121.61	ENF	Csb	-
US-Me4	Metolius-old aged ponderosa pine	USA	44.50	-121.62	ENF	Csb	(Law et al., 2001)
US-MMS	Morgan Monroe State Forest	USA	39.32	-86.41	DBF	Cfa	(Schmid et al., 2000)
US-MOz	Missouri Ozark Site	USA	38.74	-92.20	DBF	Cfa	(Gu et al., 2006)
US-NC2	NC_Loblolly Plantation	USA	35.80	-76.67	ENF	Cfa	(Noormets *et al.*, 2009)
US-Ne1	Mead - irrigated continuous maize site	USA	41.17	-96.48	CRO	Dfa	(Verma et al., 2005)-
US-Ne2	Mead - irrigated maize-soybean rotation site	USA	41.16	-96.47	CRO	Dfa	(Verma et al., 2005)
US-NR1	Niwot Ridge Forest (LTER NWT1)	USA	40.03	-105.55	ENF	Dfc	(Monson *et al.*, 2002)
US-Oho	Oak Openings	USA	41.55	-83.84	DBF	Dfa	(Deforest *et al.*, 2006)
US-PFa	Park Falls/WLEF	USA	45.95	-90.27	MF	Dfb	(Davis *et al.*, 2003, Ricciuto *et al.*, 2008)
US-SO2	Sky Oaks- Old Stand	USA	33.37	-116.62	WSA	Csa	(Hibbard et al., 2005)
US-SO3	Sky Oaks- Young Stand	USA	33.38	-116.62	WSA	Csa	(Lipson *et al.*, 2005)
US-SP1	Slashpine-Austin Cary- 65yrs nat regen	USA	29.74	-82.22	ENF	Cfa	(Powell et al., 2008)
US-SP2	Slashpine-Mize-clearcut-3yr,regen	USA	29.76	-82.24	ENF	Cfa	(Clark et al., 2004)
US-Syv	Sylvania Wilderness Area	USA	46.24	-89.35	MF	Dfb	(Desai et al., 2005)
US-Ton	Tonzi Ranch	USA	38.43	-120.97	WSA	Csa	(Ma et al., 2007)
US-UMB	Univ. of Mich. Biological Station	USA	45.56	-84.71	DBF	Dfb	(Gough *et al.*, 2008)
US-Var	Vaira Ranch- Ione	USA	38.41	-120.95	GRA	Csa	(Xu & Baldocchi, 2004)
US-WCr	Willow Creek	USA	45.81	-90.08	DBF	Dfb	(Cook *et al.*, 2004)
US-Wi4	Mature red pine (MRP)	USA	46.74	-91.08	ENF	Dfb	(Noormets et al., 2007)
VU-Coc	CocoFlux	Vanuatu	-15.44	167.19	EBF	Af	(Roupsard et al., 2006)

APPENDIX II – Lists of site characteristics

Table A II – Site characteristics derived from the FLUXNET database. R_0 is the reference respiration estimated with the *LinGPP* model formulation, LAI is the maximum seasonal leaf area index of the ecosystems (understorey and overstorey), $LAI_{MAX,o}$ is the maximum leaf area index of the solely overstorey, SoilC is the total soil carbon content, Age is the stand age, T_{mean} is the annual average mean temperature, Ndepo is the total atmospheric nitrogen deposition derived as described in the method section, u* is the median of the yearly friction velocity threshold identified at each site by using the method described in Papale et al., (2006). Sites with (*) in the column dist (disturbance) represent sites with recent disturbance according to what reported in the FLUXNET database.

SITE ID	*Tower Name*	R_0	LAI_{MAX}	$LAI_{MAX,o}$	*SoilC*	N_{depo}	*Age*	*dist*	T_{mean}	u_*
		$gCm^{-2}day^{-1}$	m^2m^{-2}	m^2m^{-2}	$kgCm^{-2}$	$kgN\ year^{-1}ha^{-1}$	years		°C	$m\ s^{-1}$
AT-Neu	Neustift/Stubai Valley	4.83	6.50	6.5	4.25	18.97		*	6.79	0.035
AU-How	Howard Springs	1.84	2.40	0.9	15.10	1.09		*	25.86	0.136
BE-Lon	Lonzee	2.23	5.62	5.6	3.70	23.12		*	10.88	0.134
BE-Vie	Vielsalm	2.47	5.10	5.1	3.82	25.22	96		8.31	0.459
BR-Sp1	Sao Paulo Cerrado	3.54	3.50	3.5	8.00	8.32			22.70	0.263
BW-Ma1	Maun- Mopane Woodland	0.67	1.10	1.1	0.50	3.54		*	22.83	0.159
CA-Ca1	British Columbia- Campbell River - Mature Forest Site	2.77	8.40	7.1		1.51	60		8.67	0.295
CA-Ca3	British Columbia- Campbell River - Young Plantation Site	3.84	6.70	3.0		1.65	21	*	9.97	0.102
CA-Gro	Ontario- Groundhog River-Mat. Boreal Mixed Wood	4.88	4.30	4.3		1.82	78	*	3.84	0.408
CA-Let	Lethbridge	1.05	0.80	0.8		3.01		*	6.66	
CA-Mer	Eastern Peatland- Mer Bleue	0.94	1.30	1.3		5.79			6.69	0.039
CA-NS1	UCI-1850 burn site	3.43	5.68	5.2	16.53	0.69	159		-1.32	0.270
CA-NS3	UCI-1964 burn site	6.10	9.81	5.3	3.64	0.69	45		-1.04	0.192
CA-NS6	UCI-1989 burn site	2.40	2.97	3.0	4.40	0.69	20		-0.25	0.261
CA-Oas	Sask.- SSA Old Aspen	3.70	5.10	2.1	1.63	1.28	85		2.10	0.346
CA-Ojp	Sask.- SSA Old Jack Pine	1.76	2.60	2.6	1.58	1.18	93		1.75	0.243
CA-Qfo	Quebec Mature Boreal Forest Site	2.14	3.70	3.7	3.50	1.45	102		2.66	0.273
CA-TP4	Ontario- Turkey Point Mature White Pine	3.56	8.00	8.0	3.70	12.17	70		8.95	0.316
CA-WP1	Western Peatland- LaBiche-Black Spruce/Larch Fen	0.76	2.61	1.3		1.15	136		3.63	0.017
CH-Oe1	Oensingen1 grass	3.83	4.85	4.9	18.30	23.67		*	9.21	0.043
CN-HaM	Haibei Alpine Tibet site	2.97	2.78	2.8	8.60	2.26		*	-5.18	0.065
CN-Ku1	Kubuqi_populus forest	0.23	0.23	0.2		3.14	8	*	11.09	0.080
CN-Ku2	Kubuqi_shrubland	0.61	0.20	0.2		3.14		*	11.57	
CN-Xi2	Xilinhot grassland site (X03)	0.88	0.25	0.3		5.88		*	5.96	
DE-Bay	Bayreuth-Waldstein/WeidenBrunnen	5.04	5.60	5.3	17.02	13.65	45		7.00	0.353
DE-Hai	Hainich	2.93	6.08	6.1	12.20	17.80	140		8.23	0.519
DE-Kli	Klingenberg	4.42	9.73	5.5	9.70	14.79		*	8.34	0.099
DE-Tha	Tharandt- Anchor Station	5.64	7.60	5.2	16.00	14.79	118	*	8.52	0.279
DK-Ris	Risbyholm	2.77	6.00	6.0		8.51		*	7.47	0.082
ES-ES1	El Saler	3.28	3.63	2.6		7.68			17.41	0.255
ES-ES2	El Saler-Sueca	1.04	5.80	5.8		7.68	75	*	18.01	0.070
ES-LMa	Las Majadas del Tietar	1.57	2.00	0.5	3.32	6.85	120	*	16.16	0.153
ES-VDA	Vall d'Alinya	1.66	1.35	1.4		12.02		*	6.51	0.069

FI-Hyy	Hyytiala	3.63	7.00	6.7	5.60	2.87	47	*	4.47	0.296
FI-Kaa	Kaamanen wetland	1.27	0.70	0.7		1.30			0.20	0.089
FI-Sod	Sodankyla	2.09	1.20	1.2	3.14	1.07			1.10	0.211
FR-Fon	Fontainebleau	2.20	5.05	5.1	10.20	23.38			11.50	0.163
FR-Gri	Grignon (after 6/5/2005)	2.16	3.34	3.3		21.09		*	11.25	0.100
FR-Hes	Hesse Forest- Sarrebourg	3.17	6.70	7.3	7.17	26.30	43		10.37	0.152
FR-LBr	Le Bray (after 6/28/1998)	3.51	4.00	2.5	10.90	14.30	39	*	13.66	0.206
FR-Lq2	Laqueuille extensive	3.26	3.00	3.0		18.23		*	7.66	0.146
FR-Pue	Puechabon	2.66	3.90	1.9	6.10	14.46	66		13.64	0.229
ID-Pag	Palangkaraya	4.53	5.60	5.6		2.19		*	26.55	
IL-Yat	Yatir	0.68	2.50	2.5	3.70	7.18	42	*	18.68	0.338
IT-Amp	Amplero (after 6/28/2004)	2.49	2.00	2.0	19.30	10.41		*	10.21	0.029
IT-BCi	Borgo Cioffi	2.28	5.80	5.8		8.98		*	16.29	0.091
IT-Cpz	Castelporziano	1.31	3.50	3.5	4.31	11.25			14.82	0.096
IT-MBo	Monte Bondone	4.82	2.82	2.8	35.00	18.78		*	5.09	0.075
IT-Noe	Sardinia/Arca di Noè	2.84	2.10	2.1	10.00	10.22	45		16.87	0.091
IT-Non	Nonantola	1.27	1.70	1.7	4.80	16.96	17	*	13.91	0.080
IT-PT1	Zerbolò-Parco Ticino- Canarazzo	2.65	4.45	2.2	4.59	18.91	14	*	14.53	0.185
IT-Ren	Renon/Ritten (Bolzano)	1.79	5.11	4.6	15.20	18.78		*	4.71	0.119
IT-Ro1	Roccarespampani 1	2.97	4.30	3.0	11.30	13.72	7	*	15.64	0.218
IT-Ro2	Roccarespampani 2	2.46	4.08	3.9	11.84	13.72	17		14.79	0.095
IT-SRo	San Rossore	2.89	4.20	4.2	2.15	16.10	57		15.44	0.201
JP-Tef	Teshio Experimental Forest	4.76	7.50	4.5		1.83		*	6.30	0.130
NL-Loo	Loobos	4.23	3.50	2.0	2.40	12.24			10.42	0.224
PT-Esp	Espirra	2.06	2.80	2.8		5.62	16		16.03	0.231
PT-Mi1	Mitra (Evora)	1.10	2.30	0.7		5.62			15.86	0.228
RU-Cok	Chokurdakh	1.20	1.50	1.5	4.35	0.20			2.62	
UK-EBu	Easter Bush- Scotland	2.00	3.90	3.9	22.95	6.27		*	9.00	
UK-Gri	Griffin- Aberfeldy-Scotland	3.72	7.00	7.0	15.00	4.54	25		7.61	0.175
US-ARb	ARM Southern Great Plains burn site- Lamont	2.66	3.25	3.3	13.51	10.71		*	16.97	0.195
US-ARM	ARM Southern Great Plains site- Lamont	0.84	2.10	2.1		11.52		*	15.57	0.075
US-Aud	Audubon Research Ranch	1.28	1.00	1.0		2.55		*	17.28	0.038
US-Bar	Bartlett Experimental Forest	3.91	4.70	5.1	15.50	6.98	70		7.15	0.050
US-Bkg	Brookings	1.63	3.00	3.0		8.57		*	8.05	0.098
US-Bn1	Bonanza Creek, 1920 Burn site near Delta Junction	1.73	3.50	3.5		0.62	89		-0.82	0.075
US-Bn2	Bonanza Creek, 1987 Burn site near Delta Junction	0.88	2.50	2.5		0.62	22	*	-0.29	0.071
US-Bn3	Bonanza Creek, 1999 Burn site near Delta Junction	0.69	1.10	1.1		0.62	10	*	-0.29	0.075
US-Bo1	Bondville	2.57	5.25	5.3		16.50		*	11.14	0.108
US-Brw	Alaska – Barrow	1.12	1.50	1.5	16.50	0.15			-1.38	0.071
US-Dk3	Duke Forest - loblolly pine	1.39	5.20	4.7	9.00	15.07	26	*	14.68	
US-FPe	Fort Peck	1.25	2.50	2.5		3.74		*	5.74	0.060
US-Fwf	Flagstaff – Wildfire	0.80	0.60	0.6	3.30	2.47		*	12.26	0.082
US-Ha1	Harvard Forest EMS Tower (HFR1)	3.26	5.20	5.2	8.80	12.27			8.16	0.392
US-Ho1	Howland Forest (main tower)	3.71	6.50	6.5	11.00	4.19	140		6.60	0.224
US-Ho2	Howland Forest (west tower)	3.59	5.60	5.6	12.00	4.19	140		6.51	

US-IB1	Fermi National Accelerator Laboratory- Batavia (Agricultural site)	1.90	5.25	5.3	6.30	14.95		*	13.83	0.010
US-KS2	Kennedy Space Center (scrub oak)	1.92	2.50	2.5	3.60	7.00		*	22.26	0.053
US-Los	Lost Creek	1.94	4.24	4.2	4.50	3.02	11		4.72	0.140
US-LPH	Little Prospect Hill	3.19	5.00	5.0	3.70	12.27			8.82	0.221
US-Me2	Metolius-intermediate aged ponderosa pine	2.15	2.80	2.7	7.90	3.45	95		6.82	0.601
US-Me3	Metolius-second young aged pine	0.90	0.52	0.5	10.00	3.45	21		8.47	0.064
US-Me4	Metolius-old aged ponderosa pine	1.28	2.10	2.1	5.56	3.45			8.32	0.034
US-MMS	Morgan Monroe State Forest	2.83	4.62	4.6	6.60	18.27			12.28	0.342
US-MOz	Missouri Ozark Site	2.09	4.20	4.2		17.17			14.87	0.224
US-NC2	NC_Loblolly Plantation	3.66	3.00	3.0		14.33	15	*	15.86	0.147
US-Ne1	Mead - irrigated continuous maize site	3.82	6.30	6.3	18.40	13.20		*	11.36	0.098
US-Ne2	Mead - irrigated maize-soybean rotation site	2.40	3.75	3.8	21.10	13.20		*	11.43	0.107
US-NR1	Niwot Ridge Forest (LTER NWT1)	3.04	5.60	5.1	16.00	3.77	102		2.46	0.308
US-Oho	Oak Openings	1.57	4.70	4.0		13.49	46	*	11.16	0.136
US-PFa	Park Falls/WLEF	3.31	4.10	4.1	20.20	4.32			4.59	0.211
US-SO2	Sky Oaks- Old Stand	1.15	3.00	3.0	0.87	3.56	78	*	13.77	0.038
US-SO3	Sky Oaks- Young Stand	0.66	1.10	1.1		3.56	4	*	15.87	0.104
US-SP1	Slashpine-Austin Cary- 65yrs nat regen	3.04	4.50	4.5	8.00	9.15	65		21.04	0.186
US-SP2	Slashpine-Mize-clearcut-3yr,regen	3.60	3.88	2.9		9.15	9	*	20.56	0.050
US-Syv	Sylvania Wilderness Area	2.80	3.80	3.8	10.47	2.55	350		5.20	0.406
US-Ton	Tonzi Ranch	1.88	2.00	0.6	4.85	1.87			17.36	0.143
US-UMB	Univ. of Mich. Biological Station	3.17	3.95	3.6	3.60	3.83	90		7.35	
US-Var	Vaira Ranch- Ione	2.15	2.50	2.5		1.87		*	15.93	0.047
US-WCr	Willow Creek	2.60	5.40	4.5	9.47	4.32	74		5.77	0.419
US-Wi4	Mature red pine (MRP)	1.17	2.80	1.8		4.18	69		10.19	0.162
VU-Coc	CocoFlux	4.44	5.65	3.0	4.25	0.39	24	*	24.76	0.188

APPENDIX III – List of acronyms and abbreviations

Table AIII – Acronyms and abbreviations

Acronyms	*Description*
CRO	Croplands
DBF	Deciduous Broadleaf Forest
E_0	Activation Energy [K]
EBF	Evergreen Broadleaf Forest
EF	Modeling Efficiency from Jannssen and Heuberger (1995)
ENF	Evergreen Needleleaf Forest
GPP	Gross Primary Production
$GPP_{lag,i}$	GPP measured *i* days before the observation day of ecosystem respiration
GRA	Grasslands
hRmax	GPP value at half saturation
IGBP	International Geosphere Biosphere Programme
K	Half saturation constant of the hyperbolic relationship between R_{ECO} and precipitation
k_2	Parameter governing the linear and exponential response of R_{ECO} to GPP
LAI_{MAX}	Maximum Leaf Area Index (Understorey + Overstorey)
$LAI_{MAX,o}$	Maximum Leaf Area Index (Overstorey)
MAE	Mean Absolute Error from Jannssen and Heuberger (1995)
MDS	Marginal Distribution Sampling
MF	Mixed Forest
N_{depo}	Total Nitrogen Depositions
NEE	Net Ecosystem Exchange
NEE_{mid}	NEE mid-day
NEE_{night}	NEE night-time
P	30-day Precipitation running average
PFT	Plant Functional Type
R_0	Respiration at reference temperature for TP Model with GPP dependency added
R_2	Parameter of exponential dependency between GPP and R_{ECO}
R_{ECO}	Ecosystem Respiration
Rmax	Plateau of the R_{ECO} response to GPP
RMSE	Root Mean Square Error from Jannssen and Heuberger (1995)
R_{ref}	Respiration at reference temperature for TP Model
SAV	Savanna
SHB	Shrublands
SoilC	Total soil stock (0-50 cm)
SWC	Soil Water Content
T_0	Constant temperature from Lloyd and Taylor (1994) at 46.02°C
T_A	Air temperature
TP Model	Temperature and Precipitation model, from Raich et al. (2000) and modified by Reichstein et al. (2003)
TP_b Model	TP biotic model, containing both the dependency on GPP and ecosystem LAI (Final model formulation)

T_{Ref}	Reference temperature (15 °C)
y_{mod}	Modeled data as a function of parameter vector
y_{obs}	Observed data
A	Response of R_{ECO} to null precipitation
Θ	Parameter vector
Σ	Weight of cost function
Ω_{LS}	Cost function

APPENDIX IV – Discussion of the 'spurious' correlation between R_{ECO} and GPP.

To understand whether our results were affected by the 'spurious' correlation between GPP and R_{ECO} as reported in FLUXNET (GPP_{FLUX}) we also perform the analysis using a 'quasi'-independent Reco and GPP estimates as described by Lasslop et al., (2010) ($R_{ECO\text{-}LASS}$ and $GPP_{LASS,}$). The method by Lasslop et al., (2009) do not compute GPP as a difference, but derive R_{ECO} and GPP from quasi-disjoint NEE data subsets. Hence, if existing, spurious correlations was minimized. The *'TP Model'* was optimized against $R_{ECO\text{-}LASS}$ and GPP_{LASS} and the Pearson's correlation coefficient between *'TP Model'* residuals and GPP_{LASS} was calculated ($r_{TPModel\text{-}GPPLASS}$) at each site and for each PFT.

At each site we compared the correlation between *'TP Model'* residuals and GPP derived exploiting the FLUXNET database ($r_{TPModel\text{-}GPPFLUX}$) with the $r_{TPModel\text{-}GPPLASS}$. The comparison was conducted by using the two sample paired sign test (Gibbons and Chakraborti, 2003). We test the null hypothesis that the median of the difference between two samples is zero, for a 5% significance level. The sign test was selected instead the t-test because avoids: (i) the normal distribution assumption; and (ii) distribution symmetry.

The paired sign test between $r_{TPModel\text{-}GPPFLUX}$ and $r_{TPModel\text{-}GPPLASS}$ indicates that the median for the differences of the populations is not statistically different from 0 ($p = 0.187$) confirming that the bias observed in the purely climate driven model it is not imputable to a 'spurious' correlation between Reco and GPP introduced by the partitioning method used in the FLUXNET database. The differences are negligible also if we consider each PFT separately as depicted by the box-plot in Fig. A-I and in Tab. A-IV.

Once the best model formulation including GPP as driver is selected we also compared the parameters of the 'LinGPP' model formulation (i.e. best model selected by the consistent Akaike Information Criterion, cAIC in Table 1) estimated using the GPP and R_{ECO} from FLUXNET and $R_{ECO\text{-}LASS}$ and GPP_{LASS}. The statistics in fitting were also compared. The results are summarized in the box-plot in Fig. AII in which k_2, R_0 and the main statistics in fitting (EF and RMSE) were schematically reported. These results showed that using the two different datasets the results are similar and the overall picture drawn using the Lasslop's method and the FLUXNET database is the same.

Table A IV– Statistics of the sign test between the Pearson's correlation coefficient calculated between residuals of TP Model and GPP computed using FLUXNET partitioning (Reichstein et al., 2005) and Lasslop's partitioning (Lasslop et al., 2010). In the third colums NS means that the median is not significantly different to 0 while * means a significance level of p<0.05. Median of diff. represent the median of differences of two populations, *p* the level of significance, df the degree of freedom (i.e. number of sites (n) -1). The definitions of different PFTs are: evergreen needleleaf forest (ENF), deciduous broadleaf forest (DBF), grasslands (GRA), croplands (CRO), savannah (SAV), shrublands (SHB), evergreen broadleaf forest (EBF), mixed forest (MF), wetland (WET).

PFT	***p***	**Median of Diff**		**df**
ENF	0.678	0.007	NS	25
DBF	0.774	0.001	NS	14
GRA	0.424	-0.015	NS	14
CRO	<0.05	-0.050	*	8
SAV	0.063	-0.064	NS	4
SHB	0.999	0.015	NS	4
EBF	0.688	0.046	NS	6
MF	0.999	-0.022	NS	7
WET	0.999	0	NS	2
All	0.1875	-0.009	NS	92

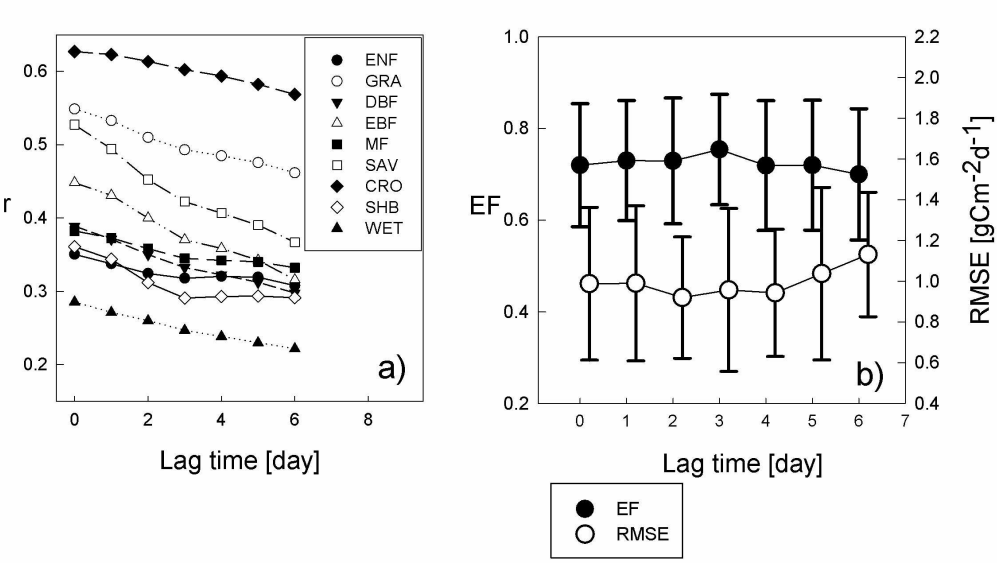

Figure 1 - a) Pearson's correlation coefficients (r) for the residual of observed minus modelled RECO versus measured GPP and a function of time lag; b) average model performances (EF and RMSE) for deciduous broadleaf forests as a function of the time lag between GPP and RECO response. Results obtained running the 'LinGPP' formulation with different GPP time series, from the GPP measured at the same day up to the GPP measured one week before the RECO. Error bars represent the standard deviation of model statistics calculated at each site. The definitions of different PFTs are: evergreen needleleaf forest (ENF), deciduous broadleaf forest (DBF), grasslands (GRA), croplands (CRO), savannah (SAV), shrublands (SHB), evergreen broadleaf forest (EBF), mixed forest (MF), wetland (WET).
191x108mm (300 x 300 DPI)

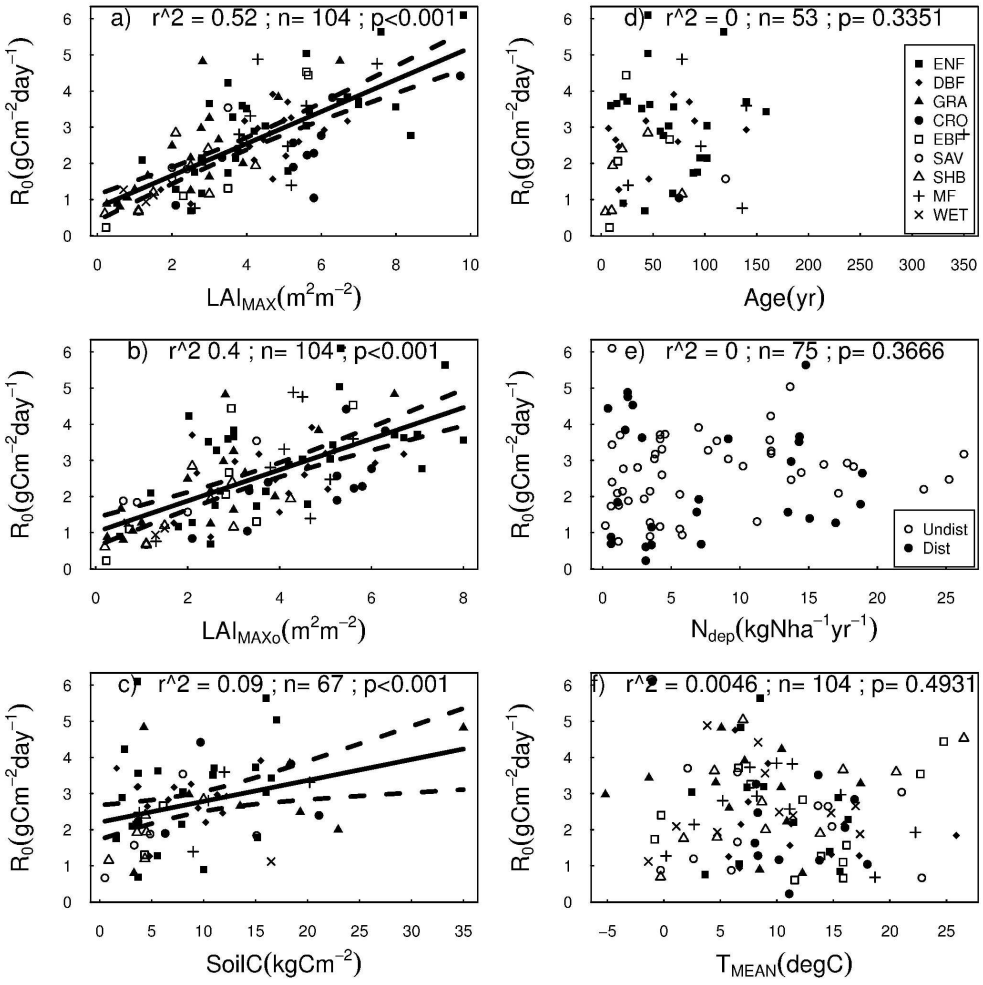

Figure 2 - Correlation between reference respiration (R0) and a) seasonal maximum leaf area index (LAIMAX) of understorey and overstorey, b) overstorey peak leaf area index (LAIMAX,o), c) total soil carbon content (SoilC), d) stand age for forest ecosystems (Age), e) total atmospheric nitrogen deposition for forest sites (Ndepo) and f) mean annual temperature. In panels a), b), c), d) and f) different symbols represent different PFT. In panel e) full circles represent disturbed sites while open circles the undisturbed ones. The r2, p and number of sites (n) were reported. The regression line and the 95% confidence interval are given if the relationship is significant. The definitions of different PFTs are: evergreen needleleaf forest (ENF), deciduous broadleaf forest (DBF), grasslands (GRA), croplands (CRO), savannah (SAV), shrublands (SHB), evergreen broadleaf forest (EBF), mixed forest (MF), wetland (WET).
177x177mm (600 x 600 DPI)

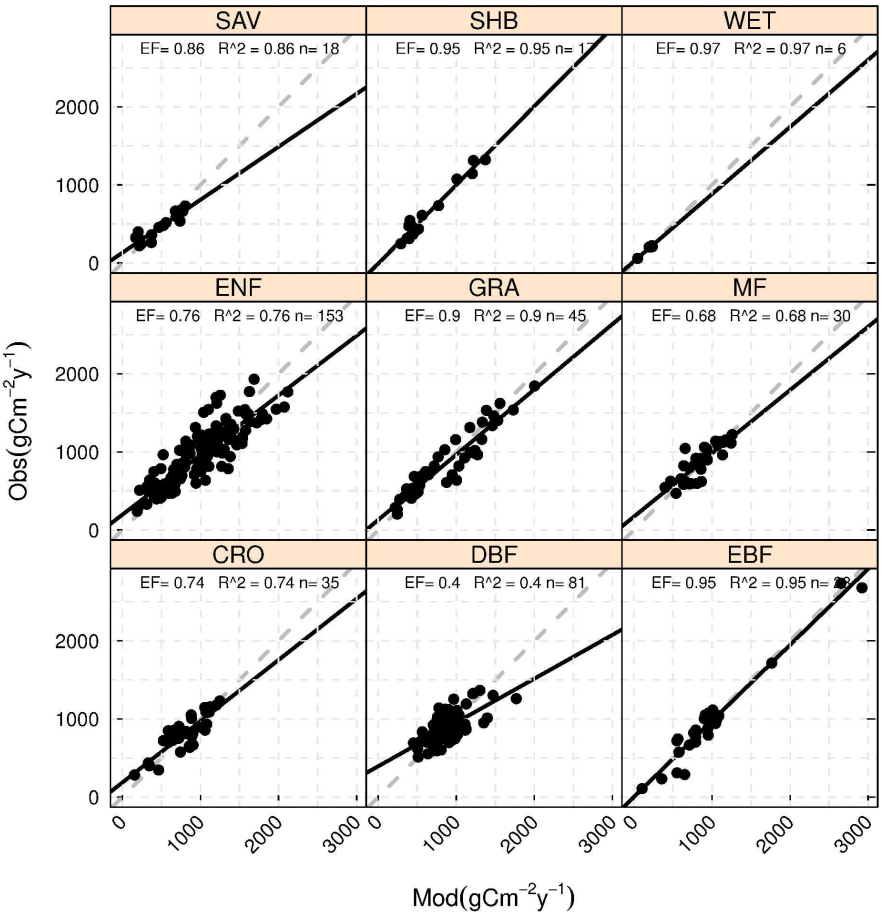

Figure 3 - Scatterplots of annual observed vs modelled RECO obtained using the 'TPGPP-LAI Model'. Each panel represent a different plant functional type (PFT). The definitions of different PFTs are: evergreen needleleaf forest (ENF), deciduous broadleaf forest (DBF), grasslands (GRA), croplands (CRO), savannah (SAV), shrublands (SHB), evergreen broadleaf forest (EBF), mixed forest (MF), wetland (WET).
177x177mm (600 x 600 DPI)

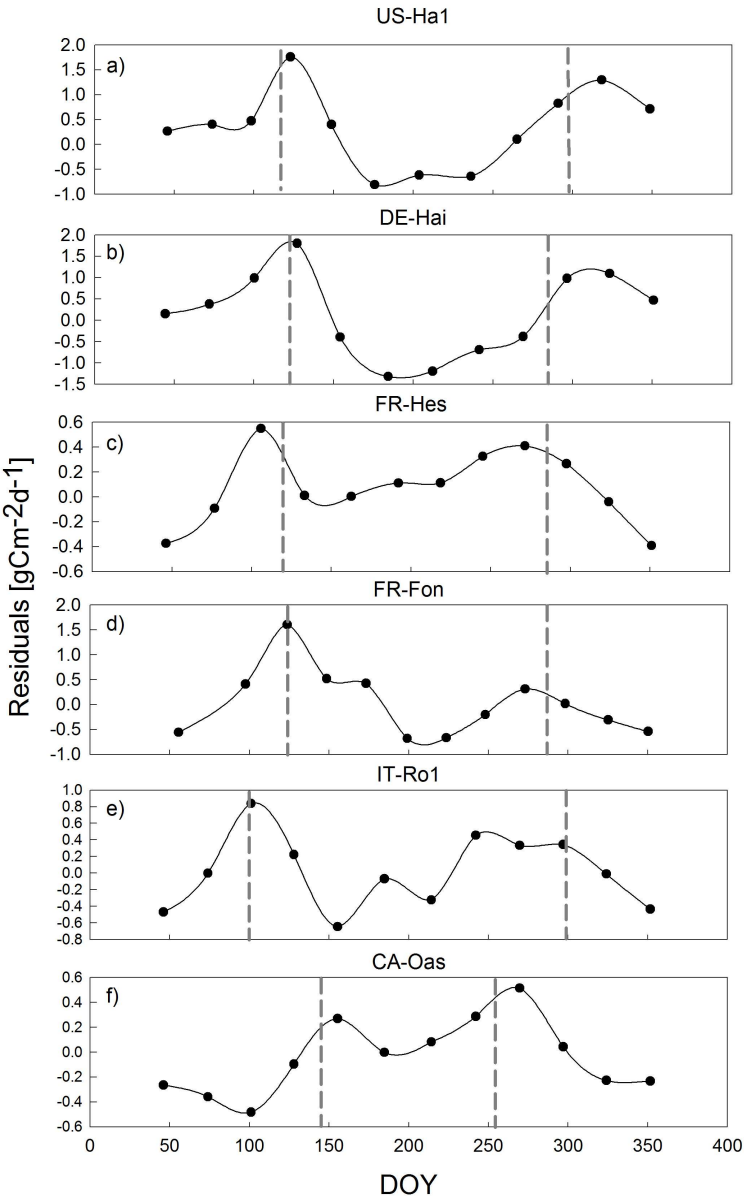

Figure 4 - Time series of average monthly model residuals for different deciduous broadleaf forest (DBF) sites. The vertical grey dashed lines represent the phenological dates. Average phenological dates were derived for US-Ha1 from literature (Jolly et al. 2005) while for other sites they were retrieved from the FLUXNET database. Average phenological dates, bud-burst and end-of-growing season are respectively: US-Ha1 (115-296),DE-Hai (126-288), FR-Hes (120-290), FR-Fon (125-292), IT-Ro1 (104-298) and CA-Oas (146-258)
379x563mm (150 x 150 DPI)

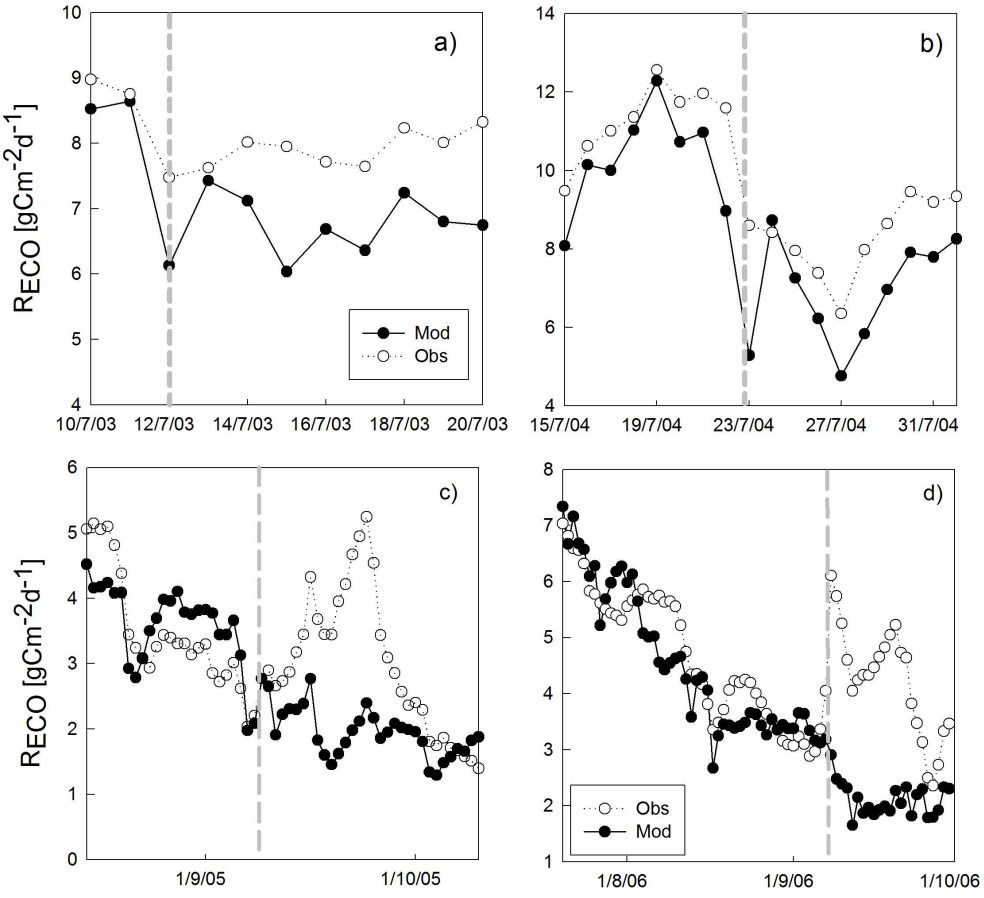

Figure 5 - Time series of observed (open circles) and modeled (black circles) for the IT-MBo site (a,b) and for the ES-ES2 site (c, d), grey dashed lines represent the dates of cuts indicated in the database (the date may be indicative), the model underestimation of fluxes in the days after each cut is clear.
382x359mm (150 x 150 DPI)

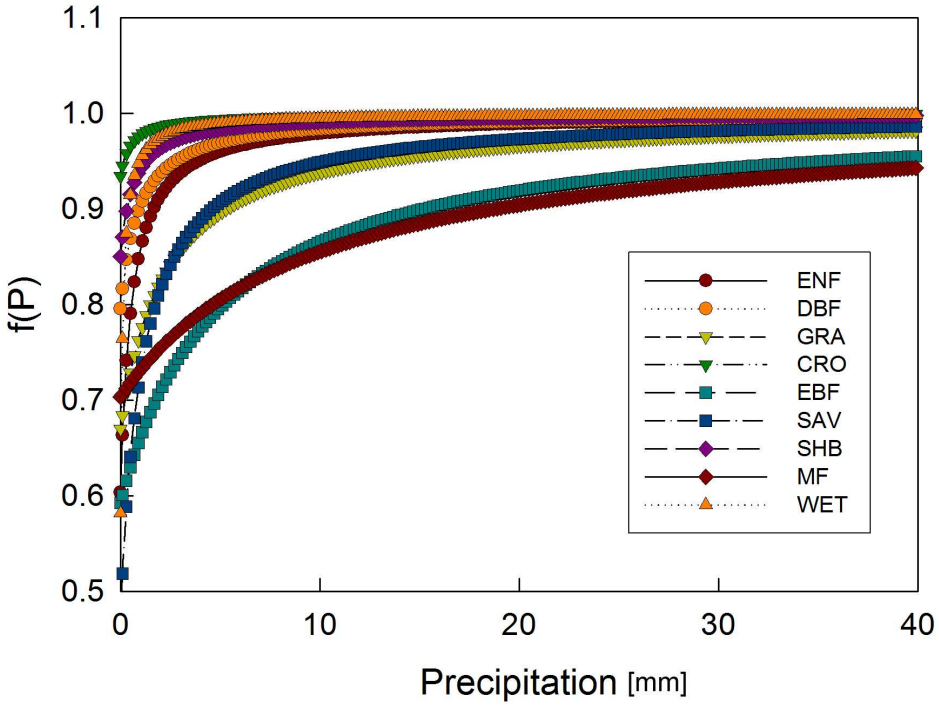

Figure 6 - Response function of ecosystem respiration to the 30-day running average of daily precipitation (Eq. 2) for each plant functional type (PFT). The parameters in Table 3 were used to draw the curves. The definitions of different PFTs are: evergreen needleleaf forest (ENF), deciduous broadleaf forest (DBF), grasslands (GRA), croplands (CRO), savannah (SAV), shrublands (SHB), evergreen broadleaf forest (EBF), mixed forest (MF), wetland (WET).
313x244mm (150 x 150 DPI)

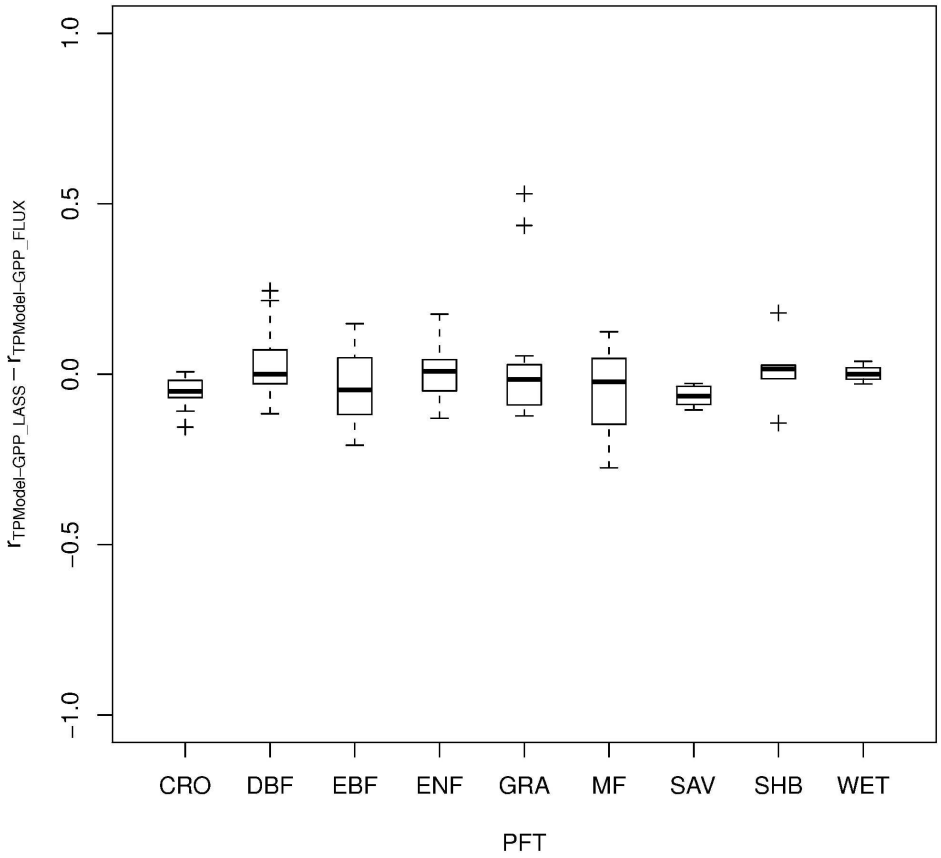

Figure AI - Box-plot of the differences at each site between the Pearson's correlation coefficient between 'TP Model' residuals and GPP computed using FLUXNET partitioning (rTPModel-GPPFLUX) and Lasslop's partitioning (rTPModel-GPPLasslop). Data were grouped in box-plots for each PFT. The definitions of different PFTs are: evergreen needleleaf forest (ENF), deciduous broadleaf forest (DBF), grasslands (GRA), croplands (CRO), savannah (SAV), shrublands (SHB), evergreen broadleaf forest (EBF), mixed forest (MF), wetland (WET)
177x177mm (600 x 600 DPI)

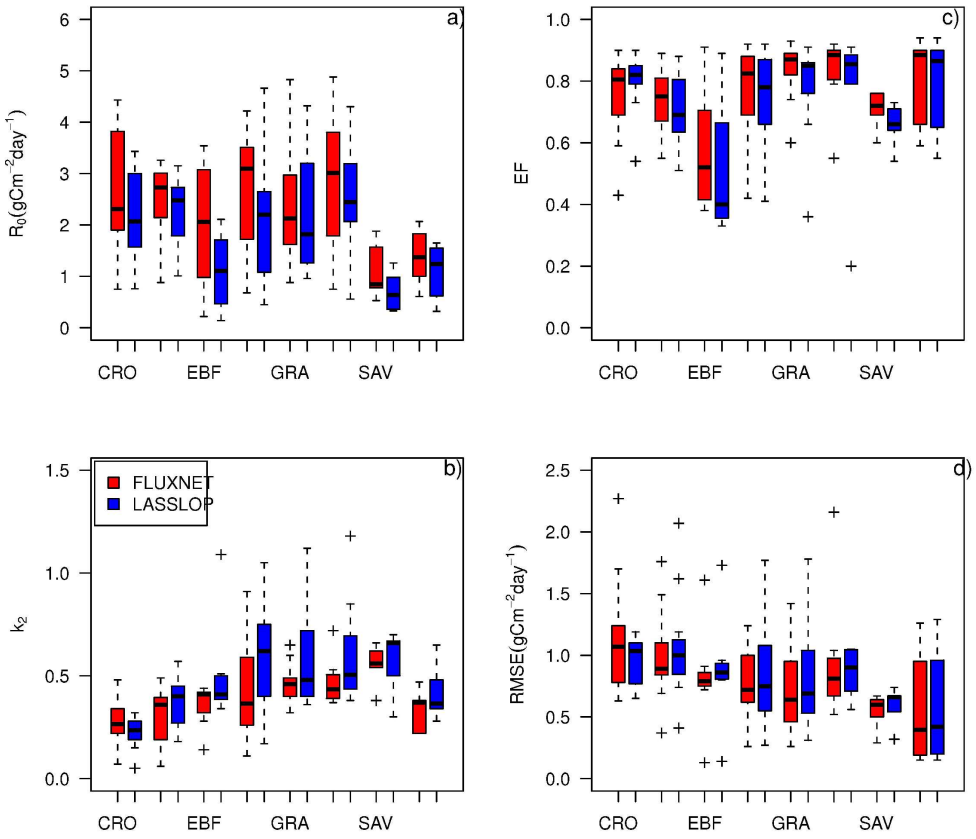

Figure AII - Box-plot of the parameters a) R0, b) k2, c) EF and d) RMSE estimated using FLUXNET (red boxes) and Lasslop's (Blue boxes) partitioning. The median of the differences of parameters governing the response to GPP (k2) estimated at each site with the two different data-sets are not statistically different from 0 except for ENF and DBF (for both $p<0.05$). No statistical differences were found for model statistics. Data were grouped in box-plots for each PFT. The definitions of different PFTs are: evergreen needleleaf forest (ENF), deciduous broadleaf forest (DBF), grasslands (GRA), croplands (CRO), savannah (SAV), shrublands (SHB), evergreen broadleaf forest (EBF), mixed forest (MF), wetland (WET).
197x177mm (600 x 600 DPI)